Pacific Journal of Mathematics

SMALL HYPERBOLIC POLYHEDRA

SHAWN RAFALSKI

Volume 255 No. 1 January 2012

PACIFIC JOURNAL OF MATHEMATICS
Vol. 255, No. 1, 2012

SMALL HYPERBOLIC POLYHEDRA

SHAWN RAFALSKI

We classify the 3-dimensional hyperbolic polyhedral orbifolds that contain no embedded essential 2-suborbifolds, up to decomposition along embedded hyperbolic triangle orbifolds (turnovers). We give a necessary condition for a 3-dimensional hyperbolic polyhedral orbifold to contain an immersed (singular) hyperbolic turnover, we classify the triangle subgroups of the fundamental groups of orientable 3-dimensional hyperbolic tetrahedral orbifolds in the case when all of the vertices of the tetrahedra are nonfinite, and we provide a conjectural classification of all the triangle subgroups of the fundamental groups of orientable 3-dimensional hyperbolic polyhedral orbifolds. Finally, we show that any triangle subgroup of a (nonorientable) 3-dimensional hyperbolic reflection group arises from a triangle reflection subgroup.

1. Introduction

Let P be a finite volume 3-dimensional hyperbolic Coxeter polyhedron. That is, P is the finite volume intersection of a finite collection of half-spaces in hyperbolic 3-space $\mathbb{H}^3$ in which the bounding planes of each pair of intersecting half-spaces meet at an angle of the form π/n, where $n \geq 2$ is an integer (the geodesic of intersection is called an *edge* of P, and the angle of intersection is called the *dihedral angle* of P along this edge). Then the group of isometries of $\mathbb{H}^3$ generated by the reflections in the faces of P is a discrete group that acts on $\mathbb{H}^3$ with fundamental domain P. Let Γ be the subgroup of index two in this reflection group generated by all the rotations of the form rs, where r and s are the reflections through two intersecting planes that support P. We denote by $\mathbb{O}_P$ the quotient space $\mathbb{H}^3/\Gamma$. Then $\mathbb{O}_P$ is an orientable hyperbolic 3-orbifold called a *hyperbolic polyhedral orbifold*. The group Γ is sometimes denoted by $\pi_1(\mathbb{O}_P)$ and called the *fundamental group of* $\mathbb{O}_P$. We call P a *hyperbolic reflection polyhedron*.

A *small* hyperbolic reflection polyhedron corresponds to a hyperbolic 3-dimensional polyhedral orbifold that contains no embedded essential 2-suborbifolds, up

MSC2010: 52B10, 57M50, 57R18.

Keywords: hyperbolic polyhedra, 3-dimensional Coxeter polyhedra, triangle groups, hyperbolic orbifold, polyhedral orbifold, small orbifold, essential suborbifold, hyperbolic turnover.

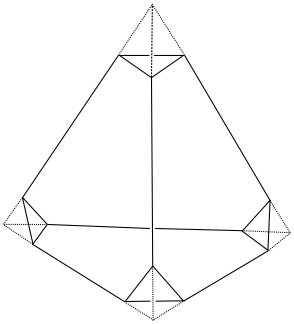

Figure 1. The small Coxeter polyhedra in $\mathbb{H}^3$.

to decomposition along embedded triangular 2-suborbifolds (Definition 2.1). We classify these polyhedra (see Figure 1):

Theorem 1.1. *A 3-dimensional hyperbolic reflection polyhedron is small if and only if it is a generalized tetrahedron.*

We also determine those hyperbolic polyhedral orbifolds that contain an immersed (singular) hyperbolic triangular 2-suborbifold. This result is a generalization of the partial classification of triangle groups inside of arithmetic hyperbolic tetrahedral reflection groups given in [Maclachlan 1996]. In Section 4, we will provide a conjectural list of all the possibilities for immersed turnovers in all polyhedral orbifolds:

Theorem 1.2. *If a hyperbolic polyhedral 3-orbifold contains a singular hyperbolic turnover that does not cover an embedded hyperbolic turnover, then at least one component of its Dunbar decomposition is a generalized tetrahedron, and the immersed turnover is contained in a unique such component. Furthermore, if T is a generalized tetrahedron with all nonfinite vertices and whose associated polyhedral 3-orbifold contains an immersed turnover, then, up to symmetry, T is of the form $T[2, m, q; 2, p, 3]$ (in the notation described in Section 4) with $m \geq 6$, $q \geq 3$ and $p \geq 6$, and the immersed turnover has singular points of orders m, q and p.*

We also determine the triangle subgroups of 3-dimensional hyperbolic reflection groups as arising from triangle reflection subgroups:

Theorem 1.3. *Any (orientable) hyperbolic triangle subgroup of a (nonorientable) 3-dimensional hyperbolic reflection group G arises as a subgroup of index two of a (nonorientable) hyperbolic triangle reflection subgroup of G.*

Essential surfaces play an integral role in low-dimensional topology and geometry. One of the most important instances of this fact is the proof of Thurston's hyperbolization theorem for Haken 3-manifolds [Thurston 1982; Morgan 1984]. In brief, Thurston's Theorem is proved by decomposing a given 3-manifold M

(which is called *Haken* if it contains an essential surface) along such surfaces as part of a finite-step process that ends in topological solid balls, from which the hyperbolic structure on M (whose existence is claimed by the theorem) is then, in a sense, reverse-engineered.

One difficulty that arises in attempting to extend the utility of essential surfaces to the orbifold setting is the possible presence of triangular hyperbolic 2-dimensional suborbifolds called *hyperbolic turnovers*. For example, whereas an irreducible 3-manifold with nonempty and nonspherical boundary always contains an essential surface, this is not always the case in the orbifold setting, with hyperbolic turnovers presenting the principal barrier. Thurston's original definition of a Haken 3-orbifold was given for nonorientable 3-orbifolds with underlying space the 3-ball and with singular locus equal to the boundary of the ball [Thurston 1979, Section 13.5, p. 324]. (The singular locus, in this instance, was meant to correspond to the boundary of a polyhedron.) Subsequent formulations of the definition of Haken ("sufficiently large" in [Dunbar 1988, Glossary] or "Haken" in [Boileau et al. 2003, Section 4.2, Remark]) were given for the orientable case and take into account the difficulties that arise from hyperbolic turnovers. Theorem 1.1, which is proved using the same observations that Thurston used to determine 3-orbifolds with the combinatorial type of a simplex as the original non-Haken polyhedral orbifolds, echoes Thurston's original result [1979, Proposition 13.5.2], with respect to this evolution of the language.

2. Definitions

There are several excellent references for orbifolds, such as [Boileau et al. 2003; Cooper et al. 2000]. All of the 3-orbifolds considered in this paper are either orientable hyperbolic polyhedral 3-orbifolds or the result of cutting an orientable hyperbolic polyhedral 3-orbifold along a finite set of totally geodesic hyperbolic turnovers or totally geodesic hyperbolic triangles with mirrored sides. A hyperbolic polyhedral 3-orbifold $\mathbb{O}_P$ is geometrically just two copies of its associated hyperbolic polyhedron P with the corresponding sides of the two copies identified. Therefore, $\mathbb{O}_P$ is a complete metric space of constant curvature -1 except along a 1-dimensional singular subset which is locally cone-like. If P is compact, $\mathbb{O}_P$ is topologically a 3-sphere together with a trivalent planar graph (corresponding to the 1-skeleton of P) with each edge marked by a positive integer to represent the submultiple of π of the dihedral angle at the corresponding edge of P. If P is noncompact with finite volume, then its ideal vertices correspond to trivalent or quadrivalent vertices in the planar graph (again, corresponding to the 1-skeleton of P) and the sum of the reciprocals of the incident edge marks at each such vertex is equal to one or two, according to whether the vertex is trivalent or quadrivalent.

In the noncompact case, $\mathbb{O}_P$ is topologically the result of taking a 3-sphere with this marked graph and removing a (closed) 3-ball neighborhood from each ideal vertex. The statements about the combinatorics of hyperbolic polyhedra in this paragraph are consequences of Andreev's Theorem [1970a; 1970b] (see also [Roeder et al. 2007; Thurston 1979, Section 13.6; 1992]).

A (closed) orientable 2-orbifold is topologically a closed orientable surface with some finite set of its points marked by positive integers (greater than one). Every such 2-orbifold can be realized as a complete metric space of constant curvature with cone-like singularities at the marked points, and where the sign of the curvature depends only on the topology of the underlying surface together with the markings. A 2-orbifold is called *spherical, Euclidean* or *hyperbolic* according to the sign of its constant curvature realization. A *turnover* is a 2-orbifold that is topologically a 2-sphere with three marked points, and a *hyperbolic turnover* is a turnover for which the reciprocal sum of the integer markings is less than one.

Although we will seldom deal with nonorientable objects, we define a *hyperbolic triangle with mirrored sides* as a topological closed disk whose boundary is marked with three distinct points, each point labeled by an integer greater than one and such that the sum of the reciprocals of these integers is less than one, and with the connecting intervals in the boundary between these points marked as "mirrors." Hyperbolic triangles with mirrored sides are nonorientable 2-orbifolds that are doubly covered by hyperbolic turnovers: they are the quotients of hyperbolic turnovers by an involution that fixes an embedded topological circle that passes through the marked points of the turnover. Every embedded hyperbolic turnover in a hyperbolic 3-orbifold can either be made totally geodesic by an isotopy in the 3-orbifold (in which case the preimage in $\mathbb{H}^3$ under the covering map of this totally geodesic 2-suborbifold is a collection of disjoint planes, each tiled by a hyperbolic triangle that is determined by the markings of the singular points — see [Maskit 1988, Chapter IX.C] or [Adams and Schoenfeld 2005, Theorem 2.1], for instance) or else can be moved by an isotopy to be the boundary of a regular neighborhood of a totally geodesic hyperbolic triangle with mirrored sides.

An embedded orientable 2-suborbifold of $\mathbb{O}_P$ is topologically a surface that meets the marked graph transversely. We note that any simple closed curve $C \subset \partial P$ that meets the 1-skeleton transversely determines such a 2-suborbifold by adjoining to C the two topological disks that it bounds, one to either side of $\partial P \subset \mathbb{O}_P$. A closed path on ∂P that is isotopic to a simple circuit in the dual graph to the 1-skeleton of P is called a *k-circuit*, where k is the number of edges the path crosses. An embedded hyperbolic triangle with mirrored sides occurs as a suborbifold of $\mathbb{O}_P$ whenever P has a triangular face all of whose edges are labeled two (in this case, the triangle with mirrored sides is topologically just the disc bounded by these three edges in the marked graph).

The terminology of this paragraph is introduced in terms of general orbifolds. A compact *n-orbifold* $\mathbb{O}$ with boundary is a metrizable topological space which is locally diffeomorphic either to the quotient of $\mathbb{R}^n$ by a finite group action or to the quotient of $\mathbb{R}^{n-1} \times [0, \infty)$ by a finite group action, with points of the latter type making up the *boundary* $\partial\mathbb{O}$ of $\mathbb{O}$ (itself an $(n-1)$-orbifold). We use the term *orbifold ball* (respectively, *orbifold disk*) to refer to the quotient of a compact 3-ball (respectively, 2-disk) by a finite group action. We say a compact 3-orbifold $\mathbb{O}$ is *irreducible* if every embedded spherical 2-suborbifold bounds an orbifold ball in $\mathbb{O}$. A 2-suborbifold $F \subset \mathbb{O}$ is called *compressible* if either F is spherical and bounds an orbifold ball or if there is a simple closed curve in F that does not bound an orbifold disk in F but that bounds an orbifold disk in $\mathbb{O}$, and *incompressible* otherwise. There is a relative notion of ∂-incompressibility (whose exact definition we do not require). We call F *essential* if it is incompressible, ∂-incompressible and not parallel to a boundary component of $\mathbb{O}$. We call a compact irreducible 3-orbifold *Haken* if it is either an orbifold ball, or a turnover crossed with an interval, or if it contains an essential 2-suborbifold but contains no essential turnover. A compact irreducible 3-orbifold is called *small* if it contains no essential 2-suborbifolds and has (possibly empty) boundary consisting only of turnovers. (We note that a compact, orientable and irreducible orbifold is both Haken and small if and only if it is either a cone on a spherical turnover or a product of a turnover with an interval.) These definitions extend to any arbitrary 3-orbifold that is diffeomorphic to the interior of a compact 3-orbifold with boundary.

We observe that Euclidean and hyperbolic turnovers are always incompressible because a simple closed curve on these objects always bounds an orbifold disk. As a consequence, in an irreducible 3-orbifold, any incompressible 2-orbifold (in fact, even any singular hyperbolic turnover) can be made disjoint from an embedded hyperbolic turnover.

Remark. It is a consequence of a theorem of Dunbar [1988] that a hyperbolic polyhedral 3-orbifold can be decomposed (uniquely, up to isotopy) along a system of essential, pairwise nonparallel hyperbolic turnovers into pieces that contain no essential (embedded) turnovers, and, moreover, that each component of the decomposition is either a Haken or a small 3-orbifold; see [Boileau et al. 2003, Theorem 4.8]. An embedded hyperbolic turnover in a hyperbolic polyhedral 3-orbifold $\mathbb{O}_P$ will correspond to a simple closed curve in ∂P that crosses exactly three edges whose dihedral angles sum to less than π. If such a curve is parallel in ∂P to a triangular face of P all of whose edges are labeled two, then the hyperbolic turnover corresponding to this curve is isotopic to the boundary of a regular neighborhood of a hyperbolic triangle with mirrored sides (the latter arising from the triangular face of P) in $\mathbb{O}_P$. In this case, one component of the Dunbar decomposition will consist of the regular neighborhood of this triangle with mirrored sides (in fact, this is a

small 3-orbifold). The complement of this component in $\mathcal{O}_P$ is (orbifold) diffeomorphic to the complement of the triangle with mirrored sides in $\mathcal{O}_P$ (because the hyperbolic turnover collapses onto the mirrored triangle as the radius of the regular neighborhood goes to zero), and so, for convenience, we discard the component of the Dunbar decomposition corresponding to this regular neighborhood.

With the above convention in mind, we have the following:

Definition 2.1. A hyperbolic reflection polyhedron P is *small* if the Dunbar decomposition of $\mathcal{O}_P$ (with the convention of the preceding paragraph) consists of a single connected small component.

In the projective model of $\mathbb{H}^3$, consider a linearly independent set of four points, any or all of which may lie on the boundary of or outside of the projective ball. If the line segment between each pair of these points intersects the interior of the projective ball, then the points determine a *generalized tetrahedron*. This polyhedron is obtained by taking the (possibly infinite volume) polyhedron in $\mathbb{H}^3$ spanned by the points and truncating its infinite volume ends by the dual hyperplanes to the superideal vertices. The resulting polyhedron has finite volume and all of its vertices are either finite or ideal. The faces arising from truncated superideal vertices — which are called, along with the finite and ideal vertices, *generalized vertices* — are triangular, and the dihedral angle at each edge of these faces is $\pi/2$. In particular, if a generalized tetrahedron P is a Coxeter polyhedron, then any generalized vertex arising from a truncated face is a hyperbolic triangle that tiles (under the tiling associated to P) a geodesic plane in $\mathbb{H}^3$ (and thus gives rise to an embedded hyperbolic triangle with mirrored sides in $\mathcal{O}_P$).

3. Proof of Theorem 1.1

Let P be a 3-dimensional hyperbolic Coxeter polyhedron, and let $\mathcal{O}_P$ be its hyperbolic polyhedral 3-orbifold. First assume that P is a generalized tetrahedron. Then $\mathcal{O}_P$ is topologically the 3-sphere with a marked planar graph as in Figure 2.

Each dot in the figure represents a generalized vertex, and so is either a finite vertex, a triangle with mirrored sides or a Euclidean turnover cusp (the latter if the vertex is ideal). Any dot that represents a triangle corresponds to a nonseparating

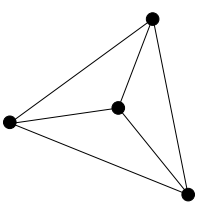

Figure 2. The graph associated to a generalized tetrahedron.

hyperbolic turnover of the Dunbar decomposition of $\mathbb{O}_P$. Moreover, since any two hyperbolic turnovers can be made disjoint by an isotopy, any other turnovers in the Dunbar decomposition occur as topological 2-spheres that intersect the graph from the figure in exactly three distinct edges. But the only possibility for such a 2-sphere is one that surrounds a dot, and that therefore is parallel to a generalized vertex of P. So the Dunbar decomposition of $\mathbb{O}_P$ (under the convention of Definition 2.1) has a single component.

To see that this component is small, we consider the graph of Figure 2 as the 1-skeleton of a tetrahedron in the 3-sphere. Using standard topology arguments, it can be shown that an incompressible 2-suborbifold intersects the interior of this tetrahedron in triangles and quadrilaterals. But a triangular intersection implies that the incompressible 2-suborbifold is isotopic to the hyperbolic turnover associated to a generalized vertex, and a quadrilateral intersection produces a compression. So P is small if it is a generalized tetrahedron.

Now assume that P is small. The rest of the proof of Theorem 1.1 depends on the following simple observation

Remark [Thurston 1979, Proposition 13.5.2]. Suppose that $C \subset \partial P$ is a simple closed curve that is transverse to, forms no bigons with, does not surround a single vertex of, and that crosses at least two distinct edges of the 1-skeleton of P. Then C determines an incompressible 2-suborbifold of $\mathbb{O}_P$ if and only if (1) it intersects any face in a connected set or not at all and (2) it intersects the common edge of two adjacent faces whenever its intersection with both faces is nonempty.

We begin with the following fact about triangular faces of P:

Lemma 3.1. *If T is a triangular face of P, then T corresponds to a hyperbolic turnover in $\mathbb{O}_P$ or P is a generalized tetrahedron.*

Proof. Suppose that T is as in Figure 3a (in this and all subsequent figures in this section, we depict P by a planar projection). If $1/p+1/q+1/r \geq 1$, then the three edges incident to the vertices of T must intersect (or meet at a Euclidean turnover)

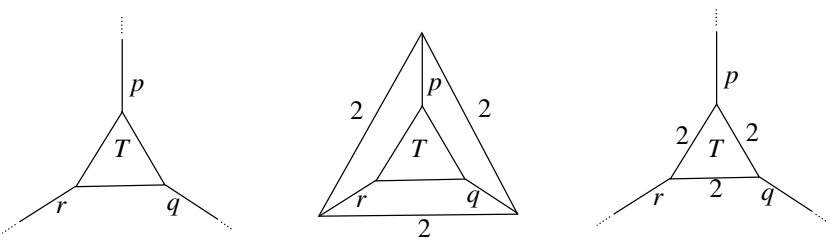

Figure 3. Triangular faces.

[Roeder et al. 2007, Lemmata 3.2 and 3.3], in which case P is a generalized tetrahedron (possibly with an ideal vertex). Otherwise, we have $1/p + 1/q + 1/r < 1$. Then the 3-circuit around this face determines a hyperbolic turnover in $\mathcal{O}_P$ whose associated triangle in P must be boundary-parallel (in P) because P is small. The two possibilities are shown in Figures 3b (in which the hyperbolic turnover collapses to the outermost face) and 3c (in which the hyperbolic turnover collapses to T). □

Throughout the rest of the proof, we will use the observation from the above lemma, i.e., that any 3-circuit in a small hyperbolic polyhedron surrounds a generalized vertex. In the case when the 3-circuit determines a hyperbolic turnover, this follows by the fact that a hyperbolic turnover in a hyperbolic 3-orbifold always corresponds to a totally geodesic 2-suborbifold (according to the second paragraph in Section 2; compare also with the incompressibility observation just before the remark on page 195): Because the polyhedron P is small, this totally geodesic 2-suborbifold of $\mathcal{O}_P$ cannot be an embedded hyperbolic turnover (because $\mathcal{O}_P$ has no boundary, and so such a turnover would have to be essential), and therefore must be a triangle with mirrored sides that corresponds to a triangular face of P.

Consider an n-sided face F of P, as in Figure 4. Assume that $n \geq 4$. The

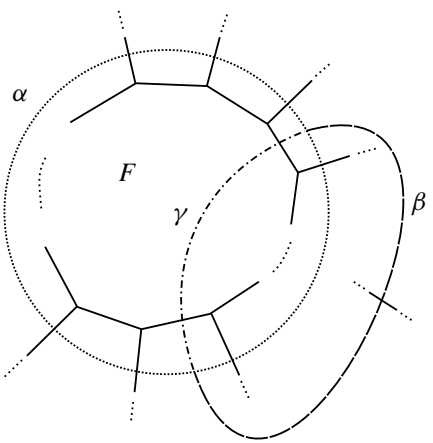

Figure 4. A face of P and a compression.

n-circuit α around F determines a 2-orbifold that must be compressible, with a compressing orbifold disk whose intersection with ∂P appears as the dashed arc β in the figure. Since $n \geq 4$, it must be that each side of the 3-circuit $\beta \cup \gamma$ contains at least two edges radiating outward from F (that is, edges meeting F only in vertices). Since $\mathcal{O}_P$ is small, $\beta \cup \gamma$ bounds a triangle $T \subset \partial P$. Figure 5 illustrates the two possibilities, depending on the side of $\beta \cup \gamma$ to which T lies. Of course, these differ only by the choice of projection of P into the plane.

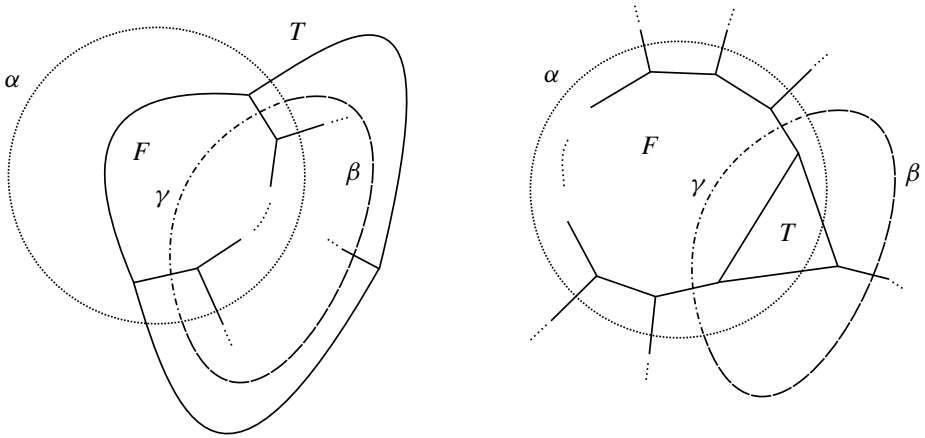

Figure 5. Two projections of a face of P with adjacent triangle.

We now consider all such compressions of this 2-orbifold, and all of the resulting adjacent triangles to F. Let α denote the k-circuit that encloses F and these triangles, as in Figure 6, left.

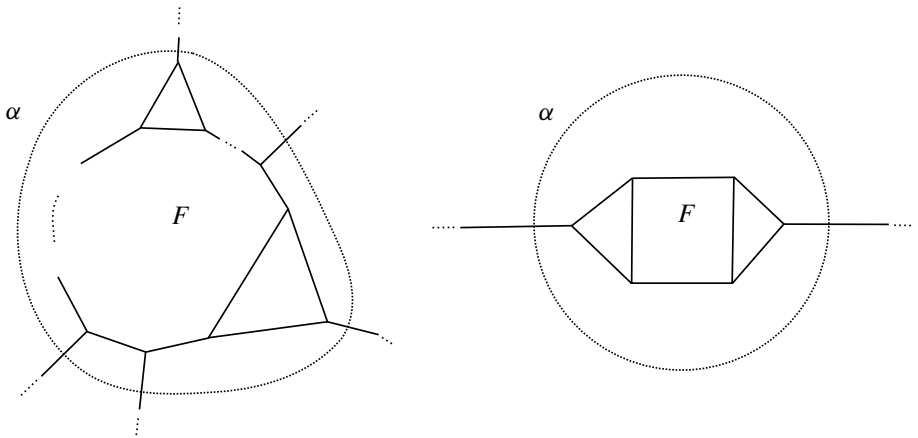

Figure 6. Left: a face of P with all of its adjacent triangles, and a k-circuit. Right: the same, with $k = 2$.

If $k = 2$, then F must be a quadrilateral with two triangles adjacent to it on opposite sides, in which case P is a triangular prism with one face that corresponds to a hyperbolic turnover in $\mathbb{O}_P$ as in Lemma 3.1, i.e., P is a generalized tetrahedron. See Figure 6, right.

If $k = 3$, then α surrounds a generalized vertex to the outside. In this case, the face F must be as in Figure 7, where each dot represents either a finite vertex, an ideal vertex or a hyperbolic triangle. Filling in the generalized vertex to the outside of α, we have that P is a generalized tetrahedron.

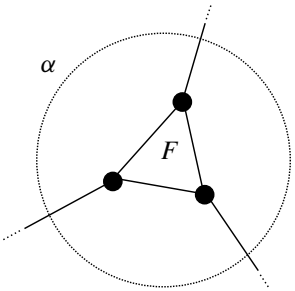

Figure 7. A face of P with all of its adjacent triangles, and a 3-circuit.

If $k > 3$, then the 2-orbifold determined by α has a compression. But any such compression would add an adjacent triangular face to F, and we have assumed that α encloses all such triangles. So $k \leq 3$. This completes the proof of Theorem 1.1.

4. Turnovers in hyperbolic polyhedra

In this final section, we prove Theorems 1.2 and 1.3, and provide a classification of the immersed hyperbolic turnovers in those tetrahedral orbifolds that arise from tetrahedra with no finite vertices. Although Theorem 1.3 does not follow from Theorem 1.2, we will provide the proof of the former in the midst of the proof of the latter, as it contains an observation that is necessary for both proofs.

It was shown in [Rafalski 2010] that if a hyperbolic 3-orbifold contains a singular hyperbolic turnover, then that turnover must be contained in a low-volume small 3-suborbifold. In particular:

Theorem 4.1 [Rafalski 2010, Theorem 1.1 and Corollary 1.3]. *Let Q be a compact, irreducible, orientable, atoroidal 3-orbifold. Then any immersion $f : \mathcal{T} \to Q$ of a hyperbolic turnover into Q is homotopic into a unique component of the Dunbar decomposition of Q, up to covers of parallel boundary components of the decomposition. Moreover, if f is a singular immersion that does not cover an embedded turnover or triangle with mirrored sides, then the component containing $f(\mathcal{T})$ is unique, and it is a small 3-orbifold.*

Proof of Theorem 1.2.. If $\mathbb{O}_P$ is a hyperbolic polyhedral 3-orbifold, then it is homeomorphic to the interior of an orbifold that satisfies the hypotheses of Theorem 4.1. If $\mathbb{O}_P$ contains a singular turnover, then this turnover is contained in a small component of the Dunbar decomposition of $\mathbb{O}_P$, and Theorem 1.1 classifies these small orbifolds as generalized tetrahedral orbifolds.

It remains to provide a classification of the generalized tetrahedra whose associated 3-orbifolds contain immersed turnovers. We will do so for generalized tetrahedra all of whose vertices are nonfinite. *See the summary at the end of the paper for the results of the classification.* The techniques we use to provide this

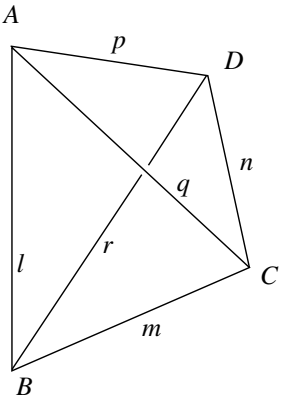

Figure 8. $T[l, m, q; n, p, r]$.

classification can be used to classify the immersed turnovers in all tetrahedral orbifolds, thereby extending and completing the classification begun by Maclachlan in the case of compact (nongeneralized) tetrahedral orbifolds [Maclachlan 1996], however, the case-by-case analysis required to complete this classification in general is somewhat excessive.

We let $T[l, m, q; n, p, r]$ denote the hyperbolic generalized tetrahedron $ABCD$ with dihedral angles π/l, π/m, π/q, π/n, π/p and π/r, as in Figure 8, with the convention that a vertex of T is truncated (respectively, ideal) if the dihedral angles of its three coincident edges sum to less than (respectively, equal to) π.

The conditions on l, m, q, n, p and r guaranteeing the existence of the tetrahedron $T[l, m, q; n, p, r]$ are known [Ushijima 2006]. In particular, there are nine compact (nontruncated) tetrahedra (see [Ratcliffe 1994, Chapter 7], for instance), all of whose associated orbifolds contain singular turnovers. We note that, of the nine compact (nontruncated) tetrahedra, eight yield arithmetic hyperbolic 3-orbifolds. As we noted above, Maclachlan classified almost all of the immersed turnovers in these arithmetic tetrahedral orbifolds using arithmetic methods. Our geometric technique can be considered as an alternative means to prove (and extend) those results, without appeal to arithmeticity.

Denote by $\mathbb{O}_T$ the 3-orbifold determined by $T[l, m, q; n, p, r]$. Recall from Section 2 that any hyperbolic turnover in a hyperbolic 3-orbifold that does not collapse onto a hyperbolic triangle with mirrored sides may be assumed to be totally geodesic. It also follows from the incompressibility of hyperbolic turnovers in irreducible orbifolds that an immersed turnover must be disjoint from any embedded turnover [Rafalski 2010, Lemma 5.3]. Consequently, if $\mathcal{T}$ is a hyperbolic turnover, then an immersion $f : \mathcal{T} \to \mathbb{O}_T$ lifts to the universal cover $\mathbb{H}^3$ as a collection of geodesic planes with some intersections — two or more of these planes will intersect whenever there is a covering transformation (i.e., an element of the

fundamental group $\pi_1(\mathbb{O}_T)$ of $\mathbb{O}_T$, which is just the group of isometries of $\mathbb{H}^3$ that yields the quotient $\mathbb{O}_T$) that does not move one plane completely disjoint from some of the others, and this must occur if there is a singular immersion of a turnover in $\mathbb{O}_T$ — and, additionally, the collection of planes determined by an immersed turnover must be disjoint from the collection of planes determined by any turnover corresponding to a generalized vertex of T.

Proof of Theorem 1.3. Let $P \subset \mathbb{H}^3$ be a polyhedron that generates the nonorientable 3-dimensional hyperbolic polyhedral reflection group G, and let $S \subset G$ be an orientable triangle subgroup. Then S is generated by two elliptic elements in G and stabilizes a plane $\Pi_S \subset \mathbb{H}^3$. In particular, Π_S meets the axis of every element of S at a right angle, and the intersections of Π_S with these axes comprise the vertex set of a tiling of Π_S by hyperbolic triangles. Every such vertex will have k lines passing through it (where k is the order of the elliptic element stabilizing the vertex) that are the perpendicular intersections with Π_S of G-translates of a face of P. This set of lines and their intersections generates a tiling of Π_S by hyperbolic triangles that corresponds to a hyperbolic triangle with mirrored sides in the nonorientable hyperbolic orbifold $\mathbb{H}^3/G$, and this 2-orbifold is covered by the hyperbolic turnover corresponding to S. Therefore, S is contained in the triangle reflection subgroup of G that corresponds to this nonorientable triangle 2-orbifold. □

We take a moment to emphasize the observation from the above proof: Any maximal (orientable) triangle subgroup of 3-dimensional hyperbolic polyhedral reflection group has as a fundamental domain a triangle whose edges are contained in the faces of the corresponding polyhedral tiling of $\mathbb{H}^3$ (the edges may intersect multiple faces of the polyhedral tiling). This fact is used in the next paragraph.

Here is the strategy for classifying the immersed turnovers of $\mathbb{O}_T$. (The proof is long, but this paragraph contains the core idea.) Let $\mathcal{T}$ be a hyperbolic turnover. Up to conjugacy, there is a unique discrete orientation-preserving group of isometries of the hyperbolic plane $\mathbb{H}^2$ corresponding to the tiling of $\mathbb{H}^2$ by copies of the triangle that determines $\mathcal{T}$ (the fundamental group $\pi_1(\mathcal{T})$ of $\mathcal{T}$). If $f : \mathcal{T} \to \mathbb{O}_T$ is an immersion, then f may be assumed to have totally geodesic image. Consider a plane $\Pi_{\mathcal{T}}$ in the collection of planes in $\mathbb{H}^3$ corresponding to $f(\mathcal{T})$. This plane is stabilized by a copy of the fundamental group of some turnover (possibly a smaller turnover that is covered by $f(\mathcal{T})$, if the fundamental group of $f(\mathcal{T})$ is not maximal) — a subgroup Γ of the fundamental group of the orbifold $\mathbb{O}_T$ — for which there is a tiling of $\Pi_{\mathcal{T}}$ by hyperbolic triangles whose edges are a (possibly proper) subset of the intersections of $\Pi_{\mathcal{T}}$ with Γ-translates of the faces of T, and whose vertices are a (possibly proper) subset of the perpendicular intersections of $\Pi_{\mathcal{T}}$ with Γ-translates of the edges of T. We will locate all of the immersed turnovers in $\mathbb{O}_T$ by reversing this process, that is, by determining exactly the hyperbolic planes in

the universal cover $\mathbb{H}^3$ that are stabilized by a triangle subgroup of $\pi_1(\mathbb{O}_T)$. Thus we choose an arbitrary edge e_1 of T and develop copies of T in $\mathbb{H}^3$ (by reflecting in faces) until we find another edge e_2 which is coplanar with but which shares no (generalized) vertex with e_1. Since we need only concern ourselves with maximal triangle subgroups, the observation following the proof of Theorem 1.3 allows to assume that the common plane, which we denote by Π_F (where F is a face of T incident to e_1), consist of developed faces of T. Let Π_1 be the plane containing another face of T incident with e_1, and let Π_2 be the plane containing another face of (a developed image of) T containing e_2. Suppose that Π_1 and Π_2 intersect Π_F at angles of π/a and π/b, respectively. If Π_1 and Π_2 intersect at an angle of π/c, and if $1/a+1/b+1/c<1$, then the rotations about edges e_1 and e_2 (of orders a and b, respectively), will generate a triangle subgroup of $\pi_1(\mathbb{O}_T)$, and the invariant plane for that subgroup will project to an immersed turnover in $\mathbb{O}_T$ (every developed edge of T that intersects the invariant plane for this triangle subgroup at an oblique angle will correspond to an immersion of the turnover). This determines a maximal triangle subgroup of $\pi_1(\mathbb{O}_T)$, and the type of the corresponding immersed turnover will be (a, b, c). In most cases, we will show that there can be no such edge e_2 that is both coplanar with e_1 and that has an incident face whose corresponding plane Π_2 intersects the plane Π_1, which rules out the possibility of an immersed turnover. In the other cases, we will find a turnover after a minimal development of T. Thus, our determination of the immersed turnovers in $\mathbb{O}_T$ will be complete.

We divide the remainder of the proof of Theorem 1.2 into subsections.

4.1. *The case when a single edge separates e_1 from e_2.*

4.1.1. *The single separating edge has order 2:* To begin, we determine the case in which the immersed turnover can be found after crossing only one edge between e_1 and e_2 (there must be at least one edge crossed, in this process, to ensure that the turnover is not parallel to a vertex). Consider Figure 9, which shows two

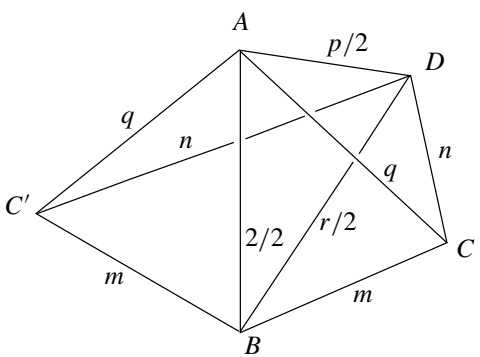

Figure 9. Two copies of the tetrahedron $T[2, m, q; n, p, r]$.

copies of the tetrahedron $T[2, m, q; n, p, r]$. Each edge is labeled according to the submultiple of π for the dihedral angle there (so, for example, the edge AD has a dihedral angle of $2\pi/p$). In particular, the points A, B, C and C' are coplanar. We use F to denote the face ABC of T and Π_F to denote the plane that contains F. We consider the edges $e_1 = AC'$ and $e_2 = BC$, and the planes $\Pi_1 = AC'D$, Π_F and $\Pi_2 = BCD$. Under the assumption that all of the vertices of T are nonfinite, we observe it is necessary for m, q, p and r to all be at least 3. From the figure, we see that Π_1 meets Π_F at an angle of π/q and that Π_F meets Π_2 at an angle of π/m, and so we are left to determine whether or not Π_1 and Π_2 intersect, and at what angle this possible intersection occurs.

The vertex D is either ideal or truncated. If it is ideal, then its link is the orbifold quotient of a horosphere by a Euclidean triangle group. If it is truncated, then it corresponds to a geodesic plane in the universal cover that is stabilized by a hyperbolic triangle group. In both cases, we illustrate the straightforward geometric determination of the conditions on n, p and r that ensure the intersection of Π_1 and Π_2 in the link of D, and determine the angle at which any intersection occurs [Rafalski 2010, Section 9.4].

Figure 10 illustrates part of the link of D *as viewed from* D (this is either a hyperbolic plane or a Euclidean plane corresponding to the horosphere centered at

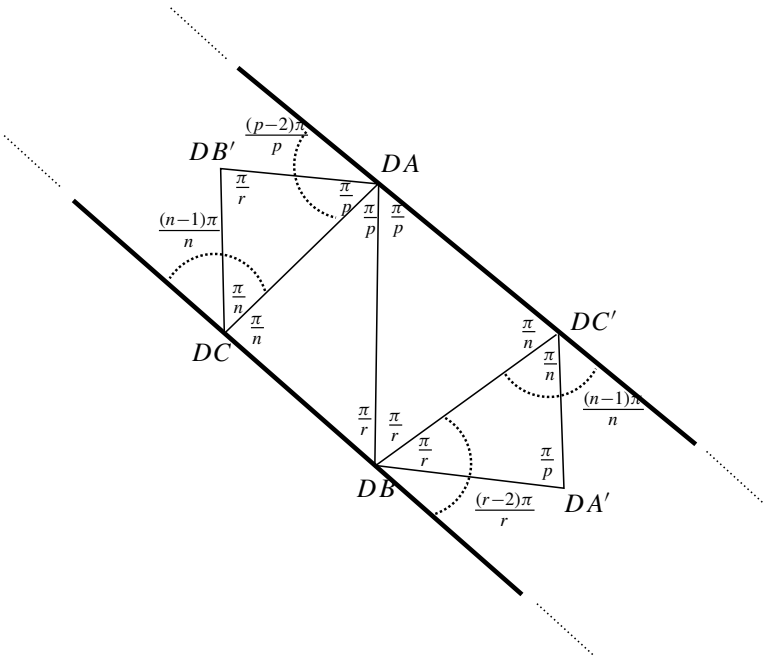

Figure 10. Part of the link of a nonfinite vertex of $T[2, m, q; n, p, r]$.

an ideal vertex). The vertices in the picture are labeled according to the edges of T that are incident at D (the labels DA' and DB' represent edges in the development of T that are the reflections of the edges DA and DB through the faces $BC'D$ and ACD, respectively, in Figure 9). Assume first that $n > 2$. Because p must be at least 3 (and similarly for r), we have the inequality $(p-2)\pi/p + (n-1)\pi/n \geq \pi$ (and similarly $(r-2)\pi/r + (n-1)\pi/n \geq \pi$). The angles with the measures from the previous sentence are indicated in the figure as the labels of the four *dotted* arcs (all other angles in the figure refer to the measure at the appropriate triangular vertex). Using this inequality, we conclude that the indicated bold rays directed northwest from DA and DC do not intersect, because the sum of the angles that these rays make with the segment from DC to DA is at least π (and similarly for the rays directed southeast from DC' and DB, because the sum of the angles that these rays make with the segment from DB to DC' is at least π). Consequently, the bold lines in the figure (and the corresponding planes Π_1 and Π_2) cannot intersect in this case. A similar argument implying that Π_1 and Π_2 do not intersect holds when $n = 2$ and both p and r are greater than 3: The rays directed northwest from DA and DC make angles with the segment between these two points of $(p-2)\pi/p \geq \pi/2$ and $\pi/2$, respectively, and so the sum of these angles will be at least π (when $n = 2$ and $r \geq 4$, the same argument proves that the southeast rays from DC' and DB do not intersect). Finally, if $n = 2$ and $p = 3$ (respectively, $r = 3$), then it is easily seen Π_1 and Π_2 intersect at an angle of π/r (respectively, π/p), and the line of intersection passes through the point DB' (respectively, DA').

We therefore have, when $l = 2$ and our search for a turnover crosses only one edge, that an immersed turnover only arises when $n = 2$ and either $r = 3$ or $p = 3$. If $r = 3$, then this yields a triple of planes intersecting pairwise in angles of π/q, π/m and π/p, with $q \geq 3$, $m \geq 6$ and $p \geq 6$. If $p = 3$, then the pairwise angles of intersection are π/q, π/m and π/r, with $q \geq 6$, $m \geq 3$ and $r \geq 6$. (The inequalities are induced by the assumption that all of the vertices of T are nonfinite.) By analyzing Table 1 (whose data is collected from [Singerman 1972]), we see that

supergroup	subgroup	index	normal	supergroup	subgroup	index	normal
$(3,3,t)$	(t,t,t)	3	Yes	$(2,3,8)$	$(3,8,8)$	10	No
$(2,3,2t)$	(t,t,t)	6	Yes	$(2,3,9)$	$(9,9,9)$	12	No
$(2,s,2t)$	(s,s,t)	2	Yes	$(2,4,5)$	$(4,4,5)$	6	No
$(2,3,7)$	$(7,7,7)$	24	No	$(2,3,4t)$	$(t,4t,4t)$	6	No
$(2,3,7)$	$(2,7,7)$	9	No	$(2,4,2t)$	$(t,2t,2t)$	4	No
$(2,3,7)$	$(3,3,7)$	8	No	$(2,3,3t)$	$(3,t,3t)$	4	No
$(2,3,8)$	$(4,8,8)$	12	No	$(2,3,2t)$	$(2,t,2t)$	3	No

Table 1. Triangle supergroups and subgroups.

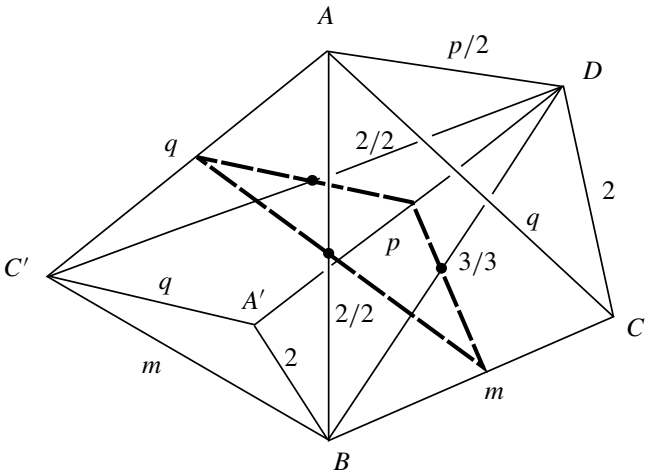

Figure 11. A (q, m, p) triangle in $T[2, m, q; 2, p, 3]$.

this triple of planes does not yield a triangle group that contains any other triangle group. By comparing the second column of the table with the first, we note that it is possible for this triple of planes to yield a triangle group that is contained in some larger triangle group. However, it is not possible for such a supergroup to be a subgroup of $\pi_1(\mathbb{O}_T)$. This follows from the observation in the paragraph following the proof of Theorem 1.3: Because such a supergroup would be a maximal triangle subgroup of $\pi_1(\mathbb{O}_T)$ stabilizing the plane that contains the (q, m, p) (or (q, m, r)) triangle, there would have to be edges in the development of T that intersect the interior of the (q, m, p) (or (q, m, r)) triangle perpendicularly (these intersections would be necessary for the corresponding orbifold covering of the smaller turnover by the larger (q, m, p) or (q, m, r) turnover). By construction, there are no such perpendicular intersections in the interior of the triangle. See Figure 11, which illustrates the case when $r = 3$. As can be seen in the figure, no developed edges of T intersect the interior of the (q, m, p) triangle (the intersections with this triangle that yield immersions of the corresponding turnover are indicated by the dots). Consequently, we can conclude that the (q, m, p) or (q, m, r) triangle determined by Π_1, Π_F and Π_2 is not parallel to any of the vertices of T, and therefore that it determines an immersed turnover in $\mathbb{O}_T$, because $\mathbb{O}_T$ is small. The observations of this paragraph are summarized in items (1) and (2) at the conclusion of the paper.

4.1.2. *The single separating edge has order 3:* We next turn to the case in which the immersed turnover can be found after crossing only one edge between e_1 and e_2, where the order of the crossed edge is $l = 3$. See Figure 12. Let $e_1 = AD'$, $e_2 = BC$, $\Pi_1 = AC'D'$ and $\Pi_2 = BCD$. We make several preliminary observations:

(1) Any two (distinct) planes that truncate developed vertices must be disjoint.

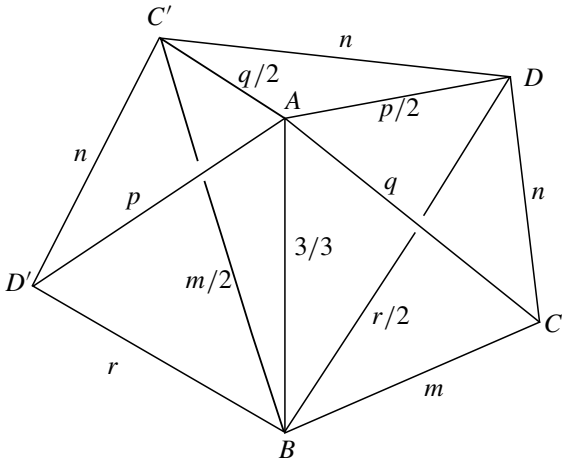

Figure 12. Three copies of the tetrahedron $T[3, m, q; n, p, r]$.

(2) By (1) and by the fact that T has no finite vertices, any two developed edges of the tetrahedron (whose corresponding geodesics in $\mathbb{H}^3$ are distinct) must be disjoint.

(3) It is always the case that the plane containing one face of a generalized hyperbolic tetrahedron will be disjoint from the plane that truncates the vertex opposite to that face.

(4) By (2), if two planes corresponding to two developed faces of T meet a third plane that corresponds to a developed face of T, then any intersection of the first two planes must occur on the side of the third plane where the two interior supplementary angles of intersection sum to less than π.

(5) Any two planes corresponding to two developed faces that both intersect a third plane that truncates a developed vertex intersect if and only if their intersections with that truncated plane (i.e., with the link of the generalized vertex) do so. A corresponding statement is also true in the case when the developed vertex is ideal, that is, that two planes corresponding to two developed faces that intersect at infinity in the case of an ideal vertex intersect in $\mathbb{H}^3$ if and only if their intersections with the link of the ideal vertex themselves intersect.

By (3), Π_2 is disjoint from the plane that truncates the vertex A. When $r = 2$, the planes Π_1 and Π_2 will intersect if and only if their intersections with the link of C' themselves intersect (by (4)). We will analyze the $r = 2$ case in a moment. When $r \geq 3$, we also have that Π_2 does not intersect the plane that truncates the vertex C', reasoned as follows. We will always choose the "inward" normal direction for a plane that contains a face of T by indicating the appropriate opposite vertex to that face in any of our diagrams. When $r = 3$, we observe that Π_2 contains the

face of the tetrahedron (not pictured in the figure) that is the reflection of $ABDC'$ through the face BDC', and so Π_2 does not intersect the truncating plane of C' in this case (by (3)). When $r \geq 4$, then we consider the line containing the segment BD which divides Π_2. The half of Π_2 that meets C is prevented from intersecting the truncating plane for C' by the plane ABD, and the other half of Π_2 is prevented from intersecting the truncating plane at C' by the plane containing the reflection of ABD through the face BDC' (both of these follow from (3)).

Therefore, when $r \neq 2$, we have that Π_2 has no intersection with the planes that truncate the vertices A and C'. We observe now that these truncating planes at A and C' determine an open ball (i.e., the region between them in $\mathbb{H}^3$) which contains Π_2. We also note that the edge from A to C' is the only segment of the line of intersection of Π_1 with the planes ABC' and ADC' that lies in this ball. Using the convention for the inward normal direction given above, we conclude that, in order for Π_1 to intersect Π_2, it is necessary for that intersection to occur on the *outward* side of either ABC' (where inward is relative to D) or the *outward* side of ADC' (where inward is relative to B), and consequently that Π_2 must cross at least one of the planes ABC' or ADC'.

By considering the geometry of the generalized vertex B, we have that Π_2 meets ABC' if and only if $r = 2$, and so we analyze this case now. In this case, $\Pi_2 = BDC'$ (as planes) and Π_1 and Π_2 intersect if and only if their intersections with the link of C' intersect (by (5)). The conditions for this intersection in the link of C' are either $m = 2$ (not possible, since $r = 2$), or $n = 2$ and one of q or m equals 3 (not possible, since $r = 2$), or else $q = 2$. In the last case, the intersection of Π_1 and Π_2 occurs along the edge $C'D$ at an angle of π/n, and because $q = 2 = r$ we must have $m \geq 6$, $p \geq 6$ and $n \geq 3$. In this case, $T = T[3, m, 2; n, p, 2]$ contains an immersed (m, n, p) turnover, and this tetrahedron (and the set of conditions on m, n and p) is isometric to the tetrahedron $T[2, p, n; 2, m, 3]$, which appears in item (1) at the end of the paper (it is listed as item (3), additionally). The summary at the end of the paper gives exact conditions on the arrangements of l, m, q, n, p and r which yield isometric tetrahedra.

Otherwise, Π_2 must intersect ADC', and any possible intersection of Π_1 and Π_2 must occur on the outward side of ADC' (that is, the side opposite to vertex B). Using the geometry of the generalized vertex D, we conclude that either $r = 2$ (the case we just analyzed), or $p = 2$, or $n = 2$ and one of p or r equals 3. If $p = 2$, then $q \geq 6$ (using the vertex A), $n \geq 3$ (using the vertex D), and $ADC' = ACDC'$ (as planes). By item (2) above, the lines AC' and CD are disjoint lines in the plane $ACDC'$. These lines are also the intersections with $ACDC'$ of Π_1 and Π_2, respectively. We consider the side of $ACDC'$ that is outward from vertex B, and the interior angles of intersection $(q - 2)\pi/q$ (formed by Π_1 and $ACDC'$) and $(n - 1)\pi/n$ (formed by Π_2 and $ACDC'$) on this side of $ACDC'$ (that is,

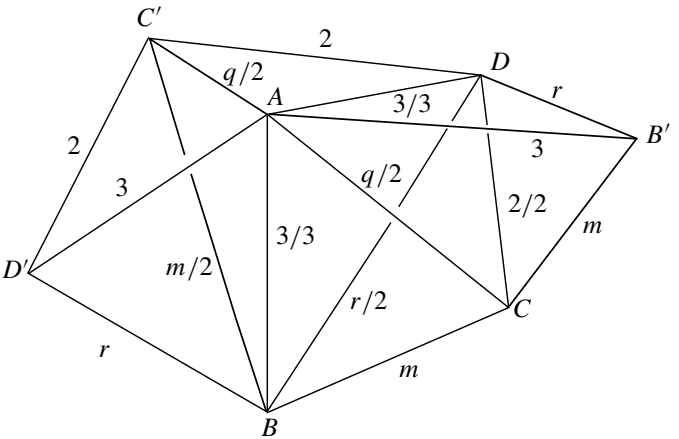

Figure 13. Four copies of the tetrahedron $T[3, m, q; 2, 3, r]$.

the two angles of intersection contained on this side of $ACDC'$ and in the same complementary component of these three planes). The conditions on n and p imply that $(n-1)\pi/n + (q-2)\pi/q \geq \pi$, and because it is only possible for Π_1 and Π_2 to intersect to the outward side of $ACDC'$ (relative to the inward B direction), we use item (4) above to conclude that $\Pi_1 \cap \Pi_2 = \varnothing$ in this case.

In the remaining case, we have $n = 2$ and one of p or r equals 3. If $p = 3$, then $r \geq 6$ and q and m must both be bigger than 2 and also satisfy $1/q + 1/m \leq 1/2$. We modify Figure 12 by adjoining another copy of T to the face ACD. See Figure 13. In this case, $ADC' = AB'DC'$ as planes, and we consider, as in the previous case, the interior angles of intersection $(q-2)\pi/q \geq \pi/3$ and $(r-1)\pi/r \geq 5\pi/6$ formed by $AB'DC'$ with Π_1 and Π_2, respectively, on the outward side of this plane (again, relative to the inward B direction). Since $(r-1)\pi/r + (q-2)\pi/q > \pi$, and again because Π_1 and Π_2 can only intersect on the side of $AB'DC'$ opposite to B, we conclude that $\Pi_1 \cap \Pi_2 = \varnothing$ in this case. The case when $n = 2$ and $r = 3$ is entirely similar, with the same conclusion.

4.1.3. *The single separating edge has order greater than 3:* We now handle the analogous cases to the previous two: when the search for an immersed turnover crosses a single edge between the planes Π_1 and Π_2, and when $l > 3$ (we will specify these planes in each example below, in an analogous way to the previous cases). We will show that no immersed turnovers can be found when $l > 3$.

We consider first the case when $l = 4$ and the vertex B has the Euclidean type $(2, 4, 4)$ with $m = 4$. See Figure 14 (we will, for the most part, drop references to the "link" of a vertex for the remainder of the paper, and assume that work done in, and figures referring to, the link of a vertex will be clear from the context). Referring to the lower half of this figure, we have $e_1 = AC''$, $\Pi_1 = AC''D'$, $e_2 = BC$

and $\Pi_2 = BCD$. The upper half of Figure 14 illustrates the view in the upper half-space model of $\mathbb{H}^3$ from the vertex B, which we have placed at the point at infinity. (This view, along with the similar figures in this section, was generated using the software *KaleidoTile* by Jeffrey Weeks [≥ 2012].) Now Π_2 is represented in this diagram by the line CD, and the plane Π_1 must be represented by a circle (the circle is the boundary of a hemisphere in this model of $\mathbb{H}^3$). We claim that the circle representing Π_1 must be centered at some point in the triangle $AC''D'$, and that none of the three points A, C'' or D' can be contained in this circle's interior. To see this, suppose first that the vertex A of the tetrahedron is a truncated vertex. Then the plane truncating that vertex would appear as a circle in the figure. This circle would have to be centered at the point labeled A because the geodesic edge from B to this plane must meet the plane perpendicularly. Next, we observe that the circle representing Π_1 must intersect the circle centered at A at a right angle (because Π_1 intersects the plane that truncates the vertex A perpendicularly). This is only possible if the point labeled A lies outside of the circle representing Π_1. In the case when the vertex A of T is an ideal vertex, then the circle representing Π_1 would pass *through* the point labeled A. Since all of the vertices A, C'' and D' of

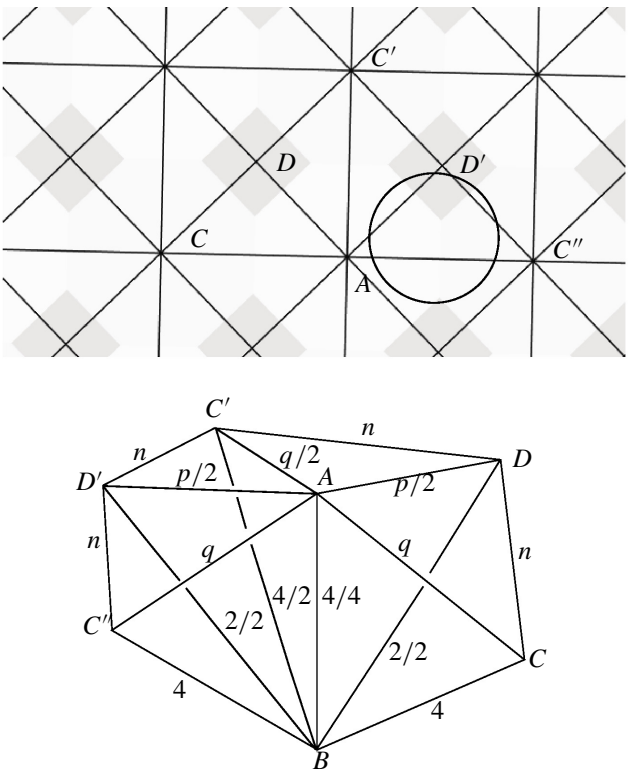

Figure 14. The view from the ideal vertex of type (2, 4, 4).

the tetrahedron are nonfinite, the circle representing Π_1 cannot contain the vertices of the triangle $AC''D'$ in its interior disk. Moreover, this circle must meet each line segment AD', AC'' and $C''D'$ (at angles of π/p, π/q and π/n, respectively) and so the center of this circle must be contained in the triangle $AC''D'$. Such a circle is depicted. Since any such circle cannot intersect the line CD, we conclude that $\Pi_1 \cap \Pi_2 = \varnothing$. An analogous argument can be used to show that we obtain no immersed turnover in this fashion, whenever the vertex B is Euclidean and l is not equal to 2 or 3; this occurs only when the triple (l, m, r) is one of $(4, 2, 4)$, $(6, 2, 3)$ or $(6, 3, 2)$.

We are left then to consider the case when $l \geq 4$ and the vertex B has a hyperbolic type. The argument is similar to the Euclidean vertex case, but we provide the details. Consider first the case of Figure 15. For the purposes of illustration, we have assumed that the vertex B has the type $(2, 4, 5)$, with $l = 5$, $m = 2$ and $r = 4$.

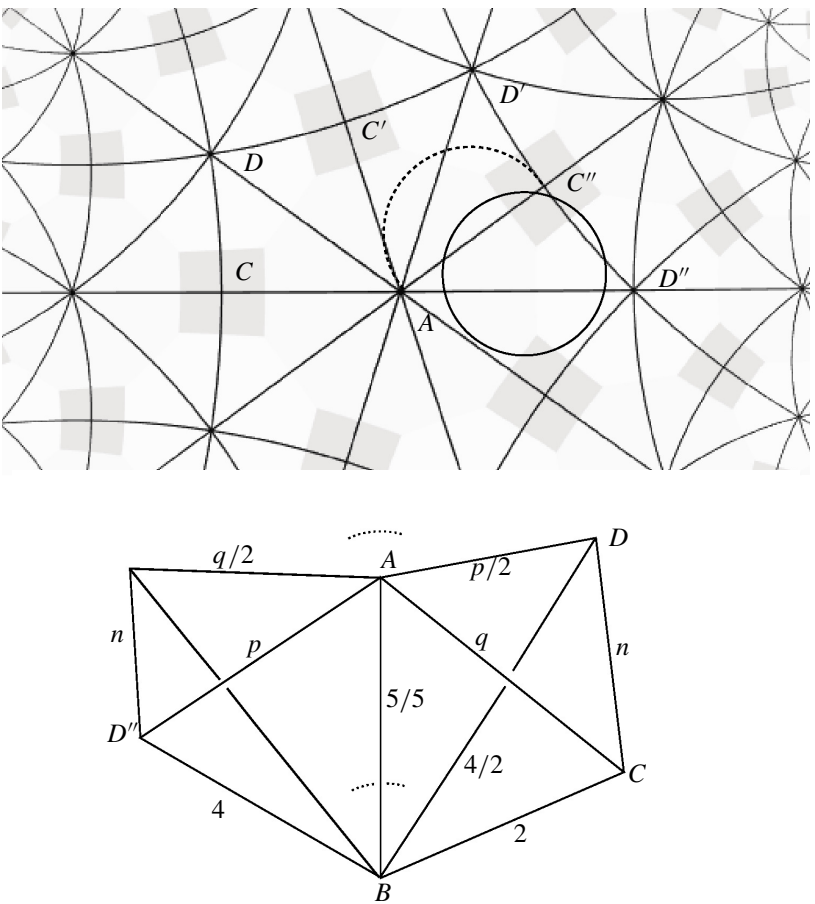

Figure 15. The view from the truncated vertex of type $(2, 4, 5)$.

Here, we have

$$e_1 = AD'', \quad \Pi_1 = AD''C'', \quad e_2 = BC, \quad \Pi_2 = BCD.$$

We consider the hyperbolic plane Π_B that truncates vertex B as a hemisphere in the upper half-plane model, and wish to construct a "view from B" that is similar to the previous case when the B was an ideal vertex. The Poincaré disk $(2, 4, 5)$ tiling pattern of the figure results from projecting this *hemi*sphere to the bounding plane of $\mathbb{H}^3$ through the south pole of the *whole* sphere that contains it [Thurston 1997, Figure 2.12, p. 58]. An important observation about this projection is that it is equivalent to projecting every point $x \in \Pi_B$ to the bounding plane of half-space along the geodesic ray that is perpendicular to Π_B at x. In particular, as in the Euclidean vertex case, each line or circular arc in the figure is the ideal boundary of a plane (each plane corresponding to a face in the tiling of $\mathbb{H}^3$ by T) that meets Π_B perpendicularly, and this projection is conformal, so that the angle of intersection between two lines or circular arcs in the figure is equal to the angle of intersection of the corresponding planes in $\mathbb{H}^3$. We have indicated, in the projection of the figure, the images of the intersection of five copies of T with Π_B, labeled the endpoints of the lines emanating from B by the corresponding letters in the lower part of the figure, and applied an isometry so that A (or, in the case that the vertex A is truncated, the center of the circle that represents the truncating plane for the vertex A) is at the center of the Poincaré disk. The planes Π_1 and Π_2 are represented by a circle and the circular arc CD, respectively.

We observe that, if the vertex C'' is truncated, then the truncating plane $\Pi_{C''}$ for C'' will appear in the figure as a circle (not pictured) with center on the segment AC'', because the point labeled C'' is the endpoint of a semicircle in the half-space model that is perpendicular to both Π_B and $\Pi_{C''}$ (to see this, recall that we may consider the projection from Π_B to the bounding plane as a projection along arcs of such semicircles). As in the previous case, the point C'' cannot be contained in the interior of the circle that is the ideal boundary of Π_1, because then the arc of the semicircle from C'' to its inverse image in Π_B under the projection would meet Π_1, and this is impossible because this arc meets $\Pi_{C''}$ perpendicularly and $\Pi_{C''}$ and Π_1 are orthogonal (the contradiction arises because it would imply the existence of a triangle with two right angles). The same argument holds when either of A or D'' is a truncated vertex, and therefore, as in the previous case, the ideal boundary of Π_1 must bound a disk whose interior is disjoint from the points A, C'' and D'' (these points may lie on the ideal boundary of Π_1 if they are ideal vertices of T). The ideal boundary of Π_1 intersects the segments AC'' and AD'' and the circular arc $C''D''$ at angles of π/q, π/p and π/n, respectively, and the center of the circle representing this ideal boundary has its center contained in the hyperbolic triangle $AC''D''$ in the projection. This is the circle that is depicted in the figure. But such

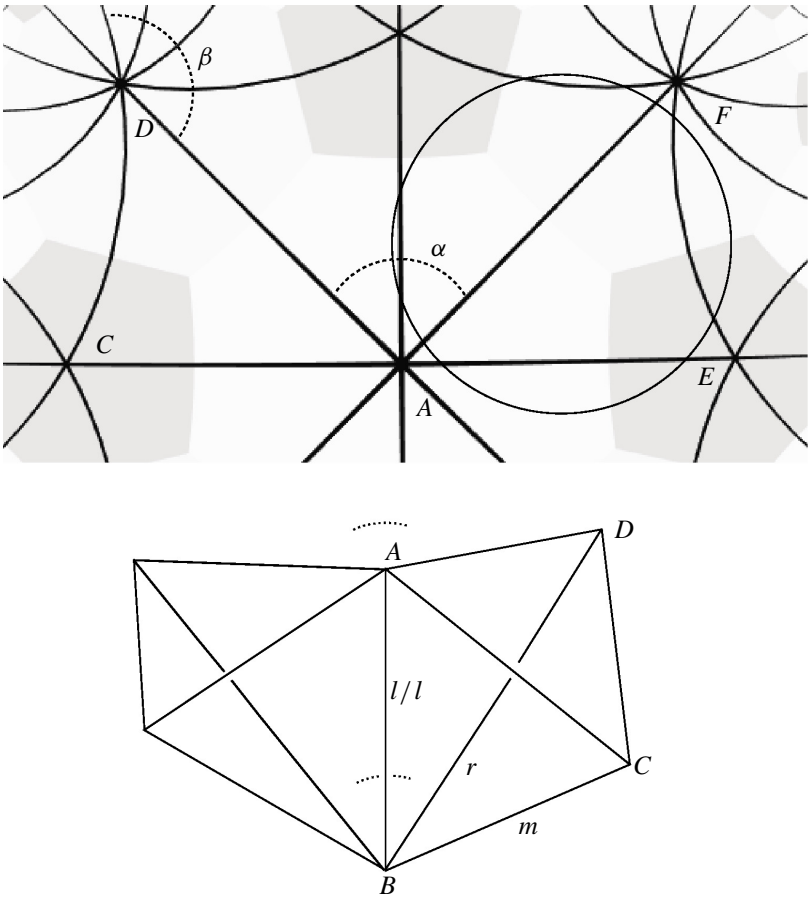

Figure 16. The view from the truncated vertex of generic hyperbolic type when none of l, m and r is 2.

a circle can have no points in the hyperbolic polygon $CAD''C''D'C'D$ that lie outside of the union of hyperbolic triangle $AC''D''$ and the circle with the segment AC'' as its diameter (pictured with a dashed arc in the figure). Consequently, this circle cannot meet any of the sides of this hyperbolic polygon other than AD'' and $D''C''$, and, in particular, we have $\Pi_1 \cap \Pi_2 = \varnothing$. An analogous argument works whenever B has hyperbolic type with one incident order 2 edge and $l \geq 4$.

The case when $l \geq 4$ and B has hyperbolic type with no incident order 2 edge is similar. See Figure 16, in which Π_2 is represented by the circular arc CD and Π_1 is represented as the circle pictured.

When $l \geq 4$, we observe that, in any similar picture (for example, Figure 17), the angles $\alpha = (l-2)\pi/l$ and $\beta = (r-1)\pi/r$ will always be at least $\pi/2$.

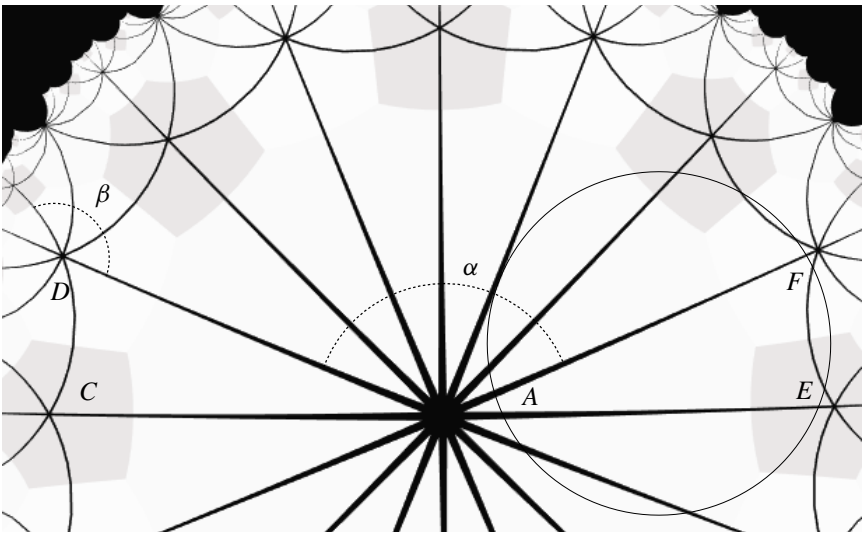

Figure 17. Another view from the truncated vertex of generic hyperbolic type when none of l, m and r is 2.

Hence, since $\alpha \geq \pi/2$ and because the center of the circle representing Π_1 is contained in the hyperbolic triangle AEF, this circle will be disjoint from the interior of the segment AD (it may pass through A, if the corresponding vertex is ideal). Also, noting that AD will always have Euclidean length equal to one of the lengths $|AF|$ or $|AE|$, the conditions on α and β imply that no point of the circle CD that lies above the line AD will be closer to the center of the circle representing Π_1 than any of the points A, E or F. Since A, E and F are not contained in the interior of this circle, we can conclude that $\Pi_1 \cap \Pi_2 = \varnothing$ in this case.

4.2. ***The case when multiple edges separates e_1 from e_2.*** Recall that $\Pi_{\mathcal{T}}$ denotes the plane stabilized by a copy of a triangle subgroup in the fundamental group of $\mathbb{O}_T$, and that e_1 and e_2 denote two developed coplanar edges of T whose (perpendicular) intersections with $\Pi_{\mathcal{T}}$ correspond to two of the cone points of an immersed turnover (whose fundamental group is the triangle group stabilizing $\Pi_{\mathcal{T}}$) in $\mathbb{O}_T$.

Notation. For the remainder of the paper, Π_F refers to the plane containing e_1 and e_2. It is the development in $\mathbb{H}^3$ of one face F of T. The diagrams from Figures 18, 19 and 20 (along with several other figures later in this section) are all drawn with the convention that Π_F is the page containing the illustration. We use L_F to denote the intersection of $\Pi_{\mathcal{T}}$ with Π_F. Additionally, the phrase "the other side of Π_F" refers, in each of the relevant figures, to the side of Π_F that is behind the page (relative to the reader), and the use of the word "plane" at any edge in a diagram *always* refers to a plane that is the development of a face of T in $\mathbb{H}^3$ that passes through that edge.

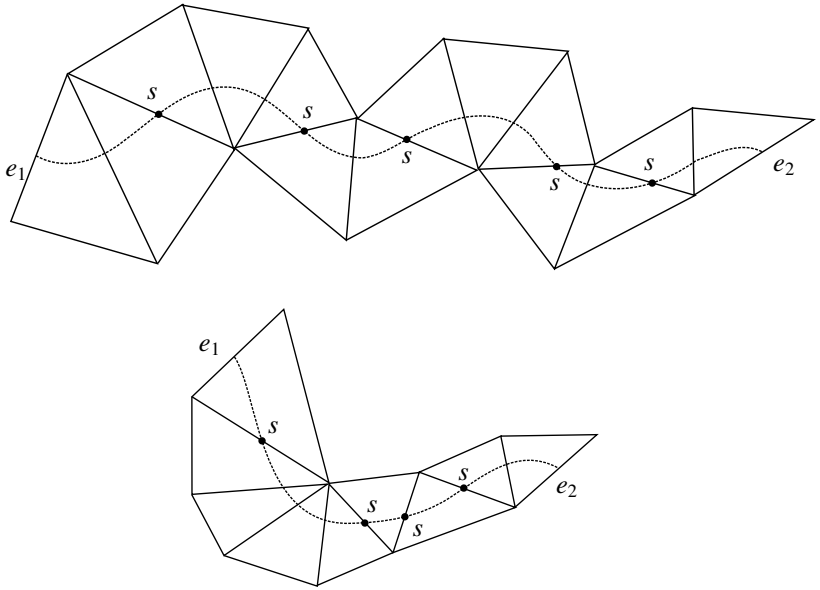

Figure 18. Schematic of some possible developments of a face of T, together with switches and the intersection of the plane $\Pi_{\mathcal{T}}$.

Now that we have determined the conditions on T which give rise to a turnover in $\mathbb{C}_T$ when $\Pi_{\mathcal{T}}$ intersects a single edge in the development of F between e_1 and e_2, we will show that it is impossible for there to be more than one such edge in the development of F between e_1 and e_2. This will complete the classification of immersed turnovers in tetrahedral orbifolds with no finite generalized vertices.

Figure 18 shows two possible schematic diagrams for this discussion. In each of the subfigures, the edges e_1 and e_2 are indicated, and the dotted line represents L_F. Notice that, in each triangle of the planar development of F, there is always a unique translate of a vertex of T that is separated from the other two by $\Pi_{\mathcal{T}}$. The edge translates of T labeled by s represent points at which this vertex switches.

We consider the following procedure for dividing any diagram of the type from Figure 18 into subdiagrams of the type (up to possible reflection or order two rotation) given in Figures 19 and 20:

(1) Starting at the first edge of the diagram, we follow L_F until we arrive at the first switch. There must always be such a switch, for otherwise the supposed turnover would be parallel to a cover of an embedded turnover corresponding to one of the truncated vertices of T.

(2) If the switch is the only switch in the diagram, then our diagram looks like, up to reflection or rotation, one of the diagrams from Figure 19. In this case, we stop.

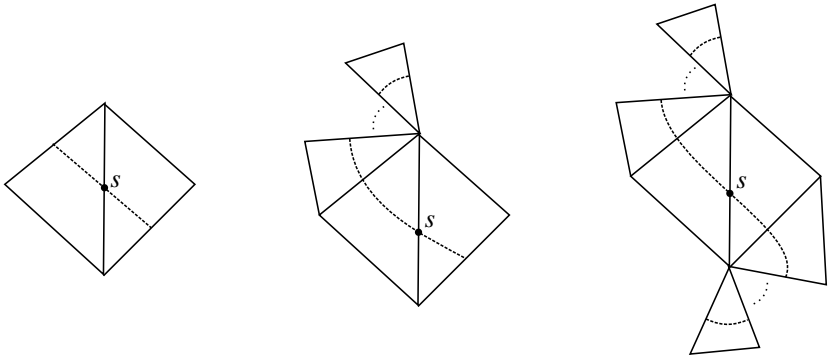

(a) (b) (c)

Figure 19. One type of possibility for the subdiagram components for a diagram of the type given in Figure 18.

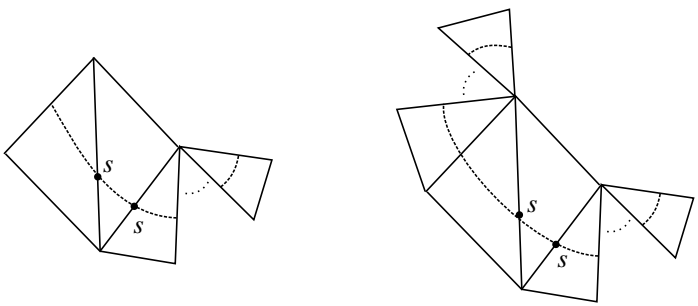

(a) (b)

Figure 20. Another type of possibility for the subdiagram components for a diagram of the type given in Figure 18.

(3) If there is more than one switch and the diagram looks like, up to reflection or rotation, one of the diagrams from Figure 20, then we stop.

(4) If we have not halted in the previous two steps, then the diagram up to and including the first edge after the first switch looks like the diagram in either Figure 19(a) or 19(b). Call this portion a *subdiagram*.

(5) Starting at the last edge of the subdiagram from the previous step, we repeat this process with the remaining portion of the original diagram, starting from the first step, until we reach edge e_2.

This procedure divides our diagram into subdiagrams of the type illustrated in parts (a) and (b) of Figure 19(a), with the possible exception that the final subdiagram may be of the type in Figure 19(c) or one of the two types in Figure 20 (we note that this process can eliminate certain switches, in each of the resulting

subdiagrams). Again, we denote by Π_1 and Π_2 the planes at e_1 and e_2, respectively, whose intersections with $\Pi_{\mathcal{T}}$ are supposed to form two of the sides of a triangle in the tiling of $\Pi_{\mathcal{T}}$. Our strategy is to use the subdiagrams of Figures 19 and 20 to find a sequence of planes in $\mathbb{H}^3$ — one or more planes at each of the two outermost edges of each subdiagram — that are pairwise disjoint on either side of Π_F and that therefore separate Π_1 from Π_2.

We first make two observations about the subdiagram from Figure 19(a). First, if either of the orders of the two edges separated by the switch is 2, then no plane at either edge can meet any of the planes at the other edge (excepting the plane Π_F). This fact follows from the extensive analysis done in Section 4.1. Second, if the two planes at the outer edges that are inclined closest toward the switch ("inclined closest" means closest, on the other side of Π_F, to the planes that pass through the switch edge) do meet (thus generating an immersed turnover in $\mathcal{O}_T$ with two singular points of order at least 6 and one singular point of order at least 3), then the next two planes (one at either outer edge) inclined away from the switch do not meet. This fact follows from an easy analysis of the patterns of line intersections in hyperbolic triangular tilings. See Figure 21 for the conditions on the vertex orders of an (a, b, c) hyperbolic triangular tiling under which such intersections can occur.

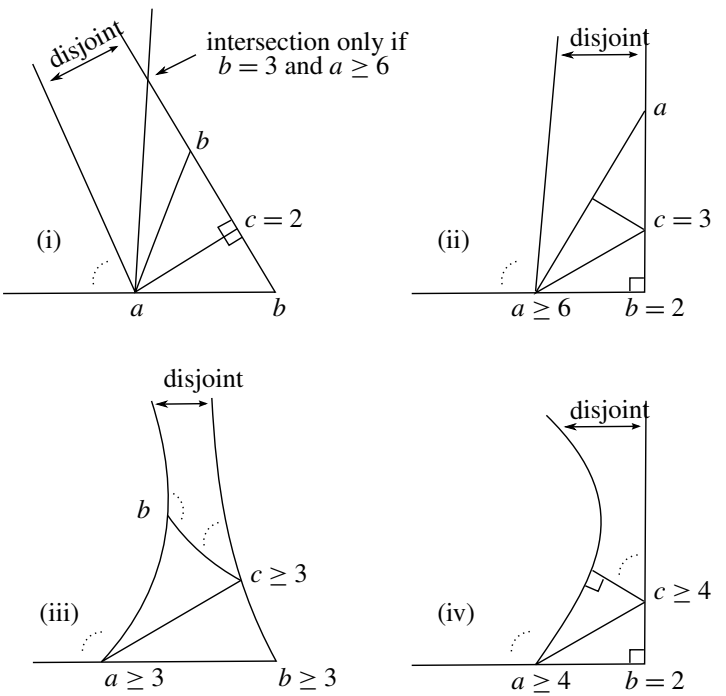

Figure 21. The possibilities for the intersection of lines in a triangular tiling of $\mathbb{E}^2$ or $\mathbb{H}^2$.

In this case (although this will not be the case for subsequent applications of this figure), Figure 21 should be thought of as depicting the plane which meets Π_F and the two southwest-to-northeast edges from Figure 19(a) perpendicularly, so that all the planes through these two edges appear as lines in Figure 21. In particular, in order for the next two planes inclined away from the switch in Figure 19(a) to meet, then one of the southwest-to-northeast edges must have order 2, which does not happen in this situation. Therefore, it is left to show that, for each of the remaining types of subdiagram, the two planes at the outer-most edges that are inclined closest to the single or double switch in the subdiagram do not intersect (again, "inclined closest" means closest, on the other side of Π_F, to the planes passing through the switch edge(s)). This will produce the sequence of planes that separates Π_1 and Π_2, and therefore complete the proof. We will show this by cases, which are indicated by their labels in the figures.

4.2.1. *Figure 19(b):* See Figure 22, in which we have supposed without loss of generality that F is the face ABC of the tetrahedron T, as in Figure 8. This picture only differs from Figure 19(b) by a 180° rotation. Observe that the edges incident at the vertices A and B have orders l, q, p and l, m, r (respectively).

We observe that the vertex B must have at least one order 2 edge incident to it. Otherwise, if B were of the type (x, y, z) with all orders at least 3, then it is readily seen, by using the information from Figure 21(iii) applied to vertex B, that Π_2 (the plane through e_2 that is inclined closest to the switch) cannot meet the plane at edge BC that is inclined closest to the switch. We indicate how this can be determined. Recall that we may construct the view from B as a triangular tiling of either the Euclidean or hyperbolic plane (in this case, a tiling by (x, y, z) triangles) such that Π_F appears as a horizontal line, and such that each edge incident to B appears as a point on that line and each plane through an edge incident to B appears as a line

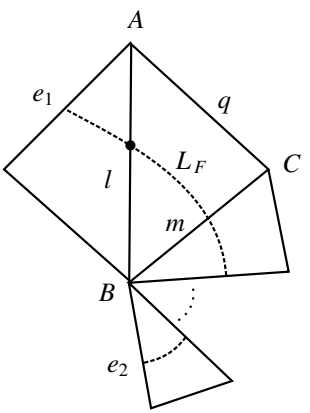

Figure 22. The case of Figure 19(b).

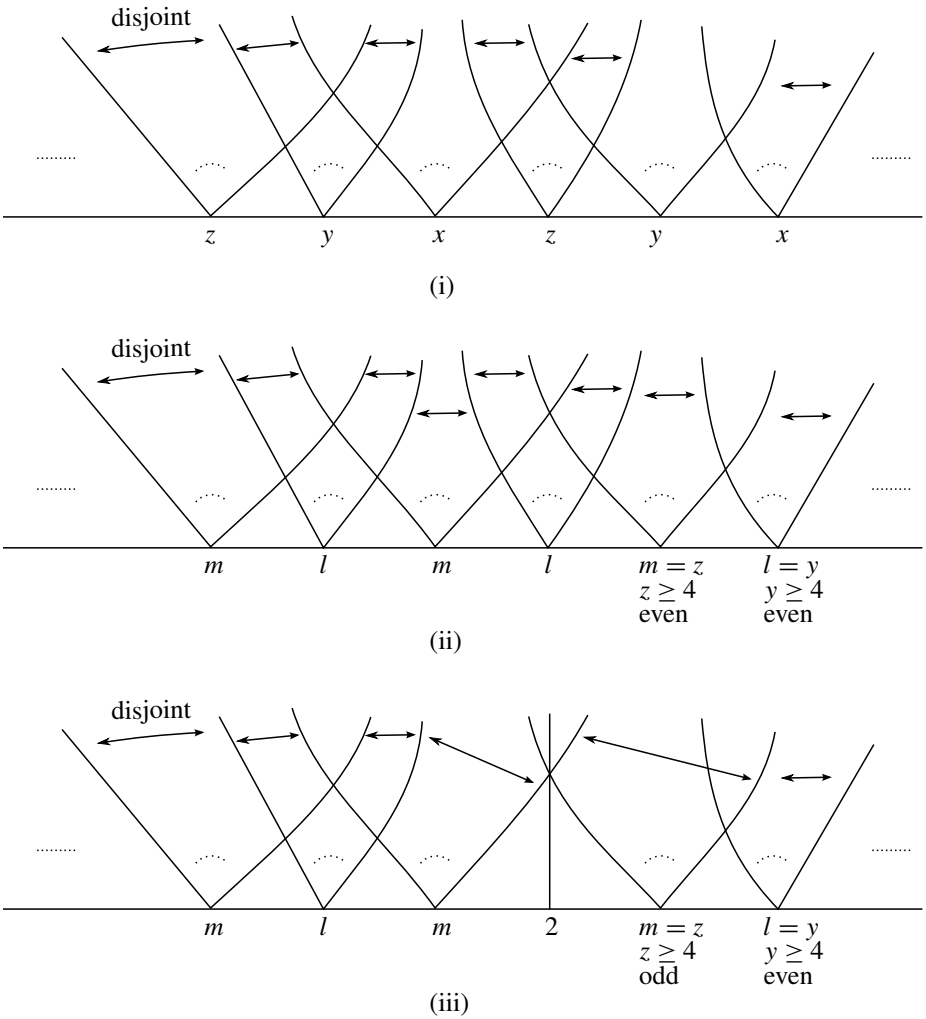

Figure 23. Patterns of intersections of certain lines corresponding to sides in a triangular tiling of $\mathbb{H}^2$ or $\mathbb{E}^2$. Double arrows indicate two lines that do not intersect above the horizontal line.

(or hyperbolic line, if B is superideal) passing through the corresponding point in the view from B. Using Figure 21(iii), we can conclude that the view from B, when B has no incident order 2 edge, looks schematically like Figure 23(i). This figure assumes that x, y and z are all odd; the other cases are similar. Suppose, for example, that the right-most point x in this figure represents the edge BC (x also indicates the order of that edge), and that the (schematic) line through this point inclined furthest to the right represents the plane through edge BC inclined closest to the switch edge AB. Then it is easily seen that no right-most inclined line through any subsequent point to the left along the horizontal can intersect with

this line. Consequently, the planes to which these lines correspond cannot intersect on the other side of Π_F (i.e., the other side of the page in Figure 22). In particular, Π_2 cannot cross the plane through BC inclined closest to the switch, as we wished to show. Furthermore, by our analysis in the cases of Section 4.1, the only way that Π_1 can meet the plane through edge BC that is inclined closest to the switch is if B has an incident order 2 edge. Consequently, if there is no such order 2 edge at B, then we have $\Pi_1 \cap \Pi_2 = \varnothing$.

So B either has the type $(2, 3, x \geq 6)$ or $(2, y \geq 4, z \geq 4)$. In the latter case, if $l = y$ or $l = z$, then we have shown in Section 4.1.3 that Π_1 is disjoint from every plane through edge BC. If $l = y$ and $m = z$ and l and m are both even, it is a simple exercise, using Figure 21(i), to show that no plane that is inclined closest to the switch edge AB through any of the subsequent edges from BC toward e_2 along L_F can meet the plane through edge BC that is inclined closest to the switch, as in the argument of the previous paragraph (the schematic of the view from B in this case would be Figure 23(ii), with the edges AB and BC corresponding to the right-most points labeled l and m, respectively). So $\Pi_1 \cap \Pi_2 = \varnothing$ in this case. If $l = y$ and $m = z$ and m is odd, we can apply the same argument (but using the information from parts (i), (ii) and (iv) from Figure 21 to obtain the schematic view from B as depicted in Figure 23(iii)) to conclude that $\Pi_1 \cap \Pi_2 = \varnothing$. The analogous cases, where $l = y$ and $m = z$ and l and m are of mixed parity, are similar. The case when $l = y$ or $l = z$ and $m = 2$ requires more analysis. Here we use the geometry of the vertex A, the fact that $l \geq 4$ and the information from Figure 21 to conclude that Π_1 cannot intersect the plane through edge AB that is inclined closest to the edge BC. But Π_1 must intersect Π_F and it must intersect some of the planes through the switch edge AB. We refer to Figure 24, which depicts the schematic view from

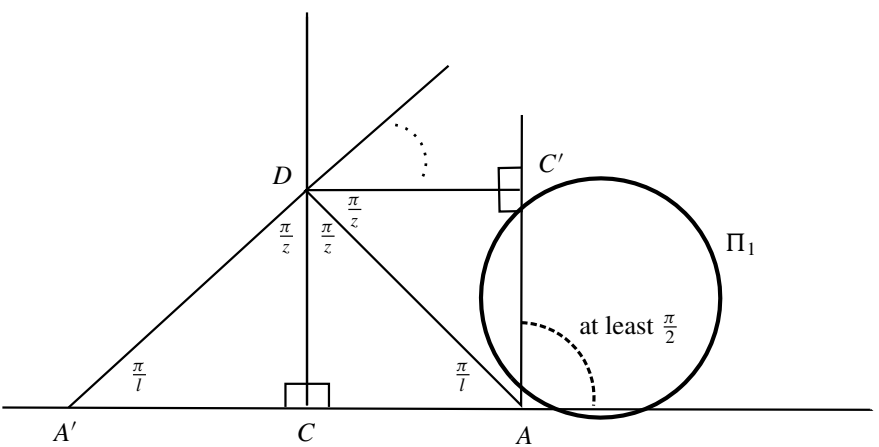

Figure 24. The schematic view from the vertex B in the case when $l = y \geq 4$, $m = 2$ and $r = z \geq 4$.

B in this case, with $l = y \geq 4$ and $m = 2$ (the third edge incident to B, which would have the label r in the tetrahedron T, is labeled by $z \geq 4$).

In this figure, the line segment AD corresponds to the plane through the switch edge AB of the tetrahedron that is inclined closest to the edge BC. As we have seen in previous cases, the ideal boundary of Π_1, in this view, is a circle that cannot contain any vertex of the triangulation in its interior disk. Since $z \geq 4$, we may conclude from the figure that the ideal boundary of Π_1 cannot intersect the line $A'D$. By noting that the line $A'D$ represents the plane inclined closest to the switch through the edge just after the edge BC along L_F toward e_2 in Figure 22, we may use the previous arguments from this paragraph to conclude that $\Pi_1 \cap \Pi_2 = \varnothing$ in this case.

Referring to the first sentence of the previous paragraph, in the latter case and when $l = 2$ and $y = 4 = z$, we may show that $\Pi_1 \cap \Pi_2 = \varnothing$ by using the Euclidean vertex argument as in Figure 14. In the latter case and when $l = 2$ and one of y or z is greater than 4, it is again readily shown that the second closest plane to the switch through edge BC (recall that Π_1 must be disjoint from this plane, by the observation of the penultimate paragraph before the start of this subsection) misses the plane inclined closest to the switch at every subsequent edge that L_F crosses toward e_2. The argument uses the information of parts (i), (ii) and (iv) from Figure 21, and is similar to the arguments already presented in the previous two paragraphs. Thus, we have $\Pi_1 \cap \Pi_2 = \varnothing$ in the case that the type of vertex B is $(2, y \geq 4, z \geq 4)$.

This leaves us with the possibility that B has type $(2, 3, x \geq 6)$. When $l = x$, we are in a case that is similar to the first case in Section 4.1.3; that is, we have to consider a regular l-gon in either the Euclidean or hyperbolic plane and a circle

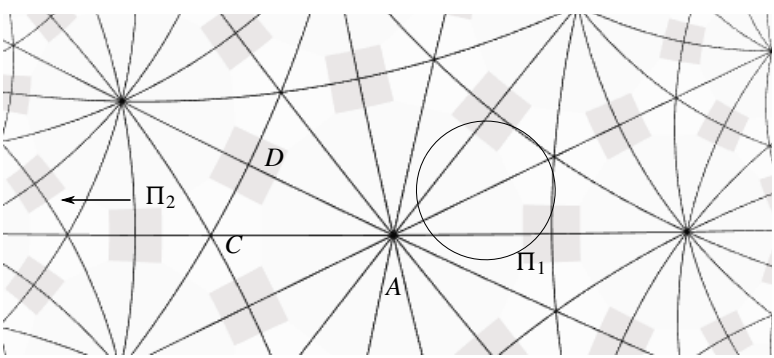

Figure 25. A view from the truncated vertex of hyperbolic type $(2, 3, 7)$. The arrow indicates that the plane Π_2 is represented by a circular arc that meets the horizontal somewhere to the left of the arc CD.

centered inside the polygon that does not contain in its interior the center of the polygon, any vertex of the polygon or any midpoint of a side. In this case, however, we observed that such a circle (representing Π_1) must be disjoint from all but two sides of the polygon. But the plane Π_2 will correspond in such a picture to a line or circular arc in the picture that does not meet the interior of this polygon, and so $\Pi_1 \cap \Pi_2 = \varnothing$ when $l = x$. See Figure 25 for an example illustration of this argument, in the case when $x = 7$.

The cases when $l = 2$ or $l = 3$ remain. In the case when $l = 3$, we refer to Figure 26. The upper half of this figure depicts the salient aspects of the view from vertex B, as in the previous cases we have considered. The lower half of the figure depicts part of the development of T in $\mathbb{H}^3$. In particular, in the lower half of the

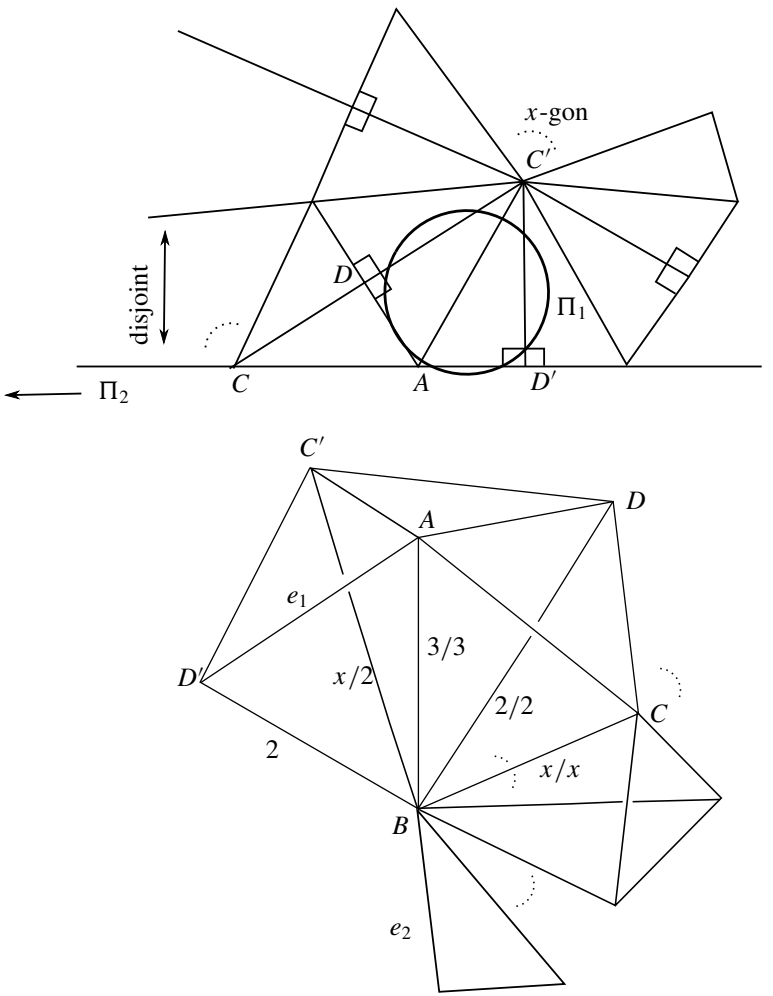

Figure 26. A view from the truncated vertex of type $(2, 3, x \geq 6)$.

figure, the triangle with edge e_2 and the lowest set of elliptical dots are both meant to lie in Π_F (which is the horizontal line CAD' in the upper half of the figure), and the plane Π_2 is not depicted, although $\Pi_1 = AC'D'$ is. In the upper half of the figure, Π_1 is represented by a circle centered at some point inside the triangle $AC'D'$ that cannot meet any vertex of the triangulation and that can only meet the sides AD and AD' of the x-gon centered at C' (the fact that this circle can meet no other sides of the x-gon centered at C' follows by an argument similar to that depicted in Figure 15 from Section 4.1.3). Since Π_2 must be represented by a line emanating from a vertex on the line CAD' which is further to the left than C (the direction, in the upper part of the figure, to which the line representing Π_2 must lie is indicated by the lower left arrow), and no such lines will enter the x-gon centered at C', we conclude that $\Pi_1 \cap \Pi_2 = \varnothing$ in this case.

When $l = 2$, then the only way for which we are unable to apply the preceding argument is when $m = 3$. See Figure 27. This is because the angle $\angle A'DC'$ is less than $\pi/2$ when $x > 6$, and so it is, in principle, possible that the circle representing Π_1 (whose center must be contained in the triangle $AC'D$) may intersect the line

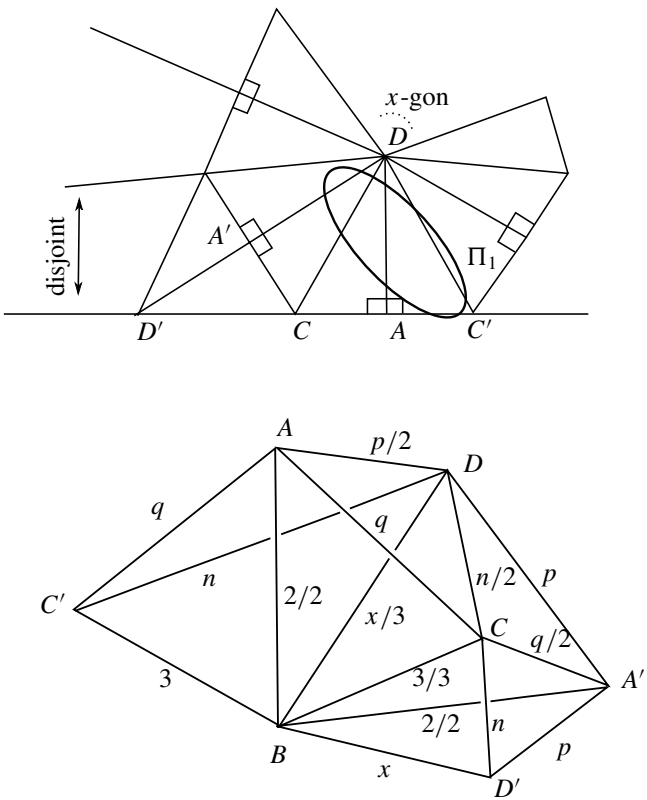

Figure 27. A view from the truncated vertex of type $(2, 3, x \geq 6)$.

representing Π_2 if $\Pi_1 = AC'D$ and $\Pi_2 = A'D'BD$ (we have drawn the circle as an ellipse in the view from B in order to indicate this possible intersection). However, using the accompanying tetrahedral illustration and the techniques of Section 4.1.1 (applied to vertex D), it is readily seen that we must have $p = 2$ and $n = 3$ in order for Π_1 and Π_2 to intersect. However, because we assume that T has no finite vertices and because $l = 2$, we do not allow $p = 2$. (*Note:* When $l = p = 2$ and $m = n = 3$ (so that the vertex A is finite), there is an immersed turnover of type (q, x, x) in T, provided that $q \geq 3$ and $x \geq 4$. See the conjectural classification at the end of this paper. In this case, $T = T[2, 3, q; 3, 2, x]$, which is isometric to the tetrahedron listed in item (6).)

4.2.2. *Figure 19(c):* See Figure 28, in which again we have supposed without loss of generality that F is the face ABC of the tetrahedron T, with the edges incident at the vertices A and B having orders l, q, p and l, m, r (respectively). We again denote by Π_1 and Π_2 the planes at the edges e_1 and e_2, respectively, that are inclined closest to the switch edge. The dotted curve in all of these figures, which we denote by L_F, represents the intersection of the planar development Π_F of F with the plane that (purportedly) contains the turnover determined by Π_F, Π_1 and Π_2.

Remark. The symbol * attached to a letter in this figure and in all subsequent figures is meant to indicate an ambiguity that may arise due to parity, and it is important for us to take note of it. For example, in Figure 28, if the order of the edge AB is even, then the vertex C^* is a developed copy of the vertex C, and the order of the edge AC^* is also q, i.e., the order of edge AC. However, if l is odd, then it would take an odd number l of tetrahedra developed around the edge AB to continue the development of the face ABC, making C^* a developed copy of the vertex D (recall that, behind the page, relative to the reader, lies the fourth vertex D of the tetrahedron), and making the order of the edge AC^* equal to p, i.e., the

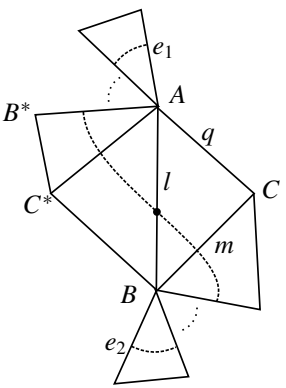

Figure 28. The case of Figure 19(c).

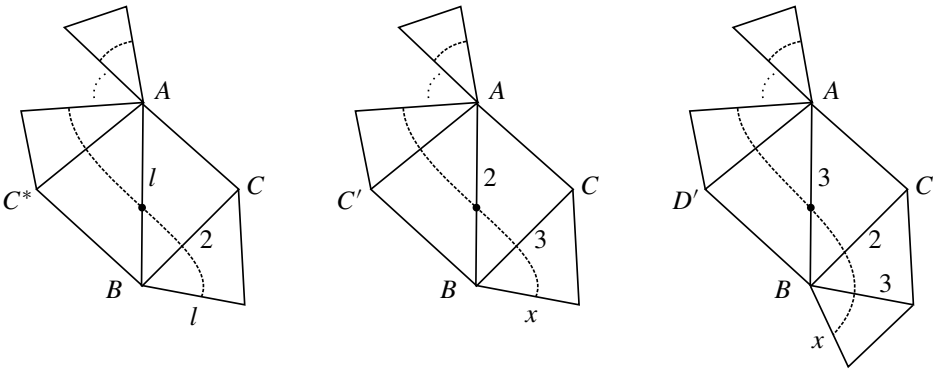

(i) $l \geq 3,\ m = 2$ (ii) $l = 2,\ m = 3,\ x \geq 6$ (iii) $l = 3,\ m = 2,\ x \geq 6$

Figure 29. After analysis, the remaining cases of Figure 19(c).

order of the edge AD (recall the notation $T[l, m, q; n, p, r]$ defined in Figure 8). We will avoid this notation whenever it is possible, although it will be necessary at times.

By the previous case, we know that Π_1 meets none of the planes through edge BC. It is therefore necessary, if Π_1 and Π_2 are to intersect, that Π_2 cross every plane through edge BC. As in the previous case, then, we can conclude that one of the edges incident at B must have order 2, for otherwise it is not possible for Π_2 to cross the plane through BC inclined closest to the switch.

Using Figure 21 and the fact that B must have an incident order 2 edge, we can reduce the cases that must be considered to those listed in Figure 29, as follows.

Referring to Figure 28, suppose first that $l = 2$ and $m = 3$. Recall that the dotted curve represents the line L_F. Then the next edge incident to B that L_F crosses after BC in the direction away from the switch should have order $x \geq 6$. A schematic of the view from B is pictured in Figure 30(i). The bold line in the figure represents *any* plane through a subsequent edge incident to B that L_F crosses after the edge with order x. Because the angle α, which is formed by the bold line and the line AC, will always be at least π/x, we conclude that the two lines indicated in the figure by the endpoints of the double arrow will not intersect above the line AC. Consequently, because the line AC represents the plane Π_F, we conclude that the planes represented by these lines will not intersect on the other side of Π_F (recall that the other side of Π_F refers to the side underneath the page in Figure 28). Therefore, we have reduced the case of showing that $\Pi_1 \cap \Pi_2 = \varnothing$ in Figure 28 to the case of Figure 29(ii), provided that $l = 2$ and $m = 3$. The case when $l = 2$ and m is even with $m \geq 4$ can be eliminated in an entirely similar fashion. See Figure 30(ii), which shows the pattern of intersections of lines that

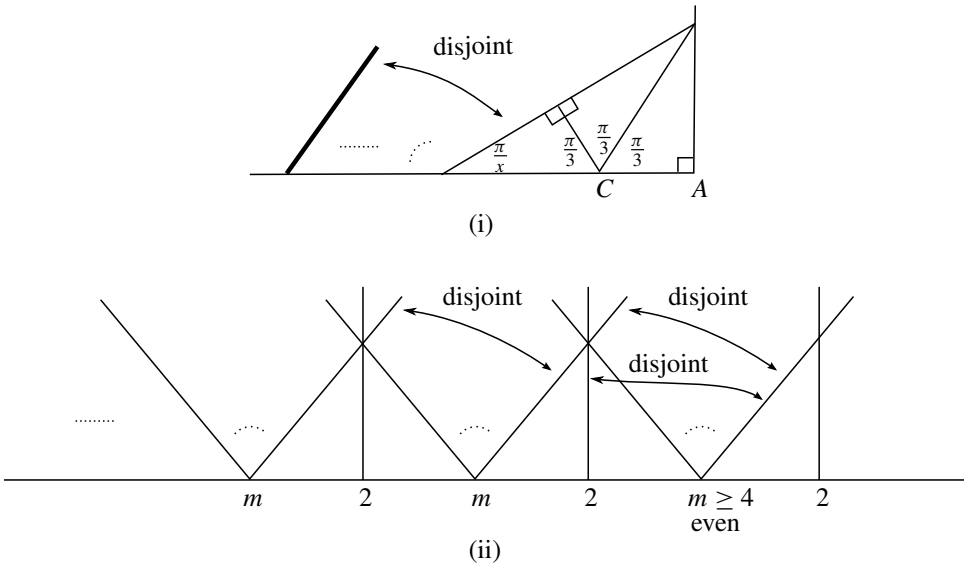

Figure 30. Patterns of intersections of certain lines corresponding to sides in a triangular tiling of $\mathbb{H}^2$ or $\mathbb{E}^2$. Double arrows indicate two lines that do not intersect above the horizontal line.

would result in the view from B. Here, we consider the right-most point on the horizontal (the horizontal represents Π_F in the view from B) with the label 2 as corresponding to the edge AB, and the right-most point on the horizontal with the label m as corresponding to the edge BC. It is readily seen from the figure that no lines passing through the labeled points on the horizontal to the left of the right-most point labeled m ever intersect the line through the latter point that is inclined closest to the switch point (i.e., the right-most point labeled 2). Therefore, no plane through an edge incident to B that is crossed by L_F after the edge BC can intersect the plane through BC inclined closest to the switch, when $l = 2$ and m is even and at least 4. Therefore, no plane through an edge incident to B that is crossed by L_F after the edge BC (such as Π_2) can intersect the plane Π_3 through BC inclined closest to the switch, when $l = 2$ and m is even and at least 4. Since Π_1 will also be disjoint from Π_3 (by Section 4.2.1), Π_1 will be separated from Π_2 by Π_3, which eliminates this case. In fact, all of the other reductions are arrived at in this way, that is, by using the information in Figure 21. The other cases that are *eliminated* by the methods of this paragraph are: (1) $l = 2$ and $m \geq 5$ with m odd, (2) $l = 3$ and $m \geq 6$ and (3) $l \geq 6$ and $m = 3$. The other cases that are *reduced* by the methods of this paragraph are: (4) $l \geq 3$ and $m = 2$ (which reduces to the case of Figure 29(i)) and (5) $l = 3$ and $m = 2$ (which reduces to the case of Figure 29(iii)). (We note that, when $l = 3$ and $m = 2$, case (i) of Figure 29 may seem to rule out case (iii).

However, the plane inclined closest to the switch through the edge labeled x in case (iii) intersects the plane inclined closest to the switch through the lower edge labeled 3 (this may be seen using the information of Figure 21). We therefore must show that $\Pi_1 \cap \Pi_2 = \varnothing$ in *both* the case that e_2 is the lower edge labeled $l = 3$ in (i) *and* in the case that e_2 is the lower edge labeled x in (iii).)

Now, we apply the arguments of the previous two paragraphs to the other direction along L_F from the switch. Specifically, referring to Figure 28, we know by the previous case that Π_2 meets none of the planes through the edge AC^*, and so we reduce the possibilities for the number of developed faces around the vertex A using the fact that Π_1 must intersect every plane through the edge AC^* in order for it to be possible for Π_1 and Π_2 to have nonempty intersection. The result of this further analysis leaves us to consider only the cases of Figure 31. We note the change from "$l \geq 3$" to "$l \geq 3$ odd" that occurs when reducing Figure 29(i) to

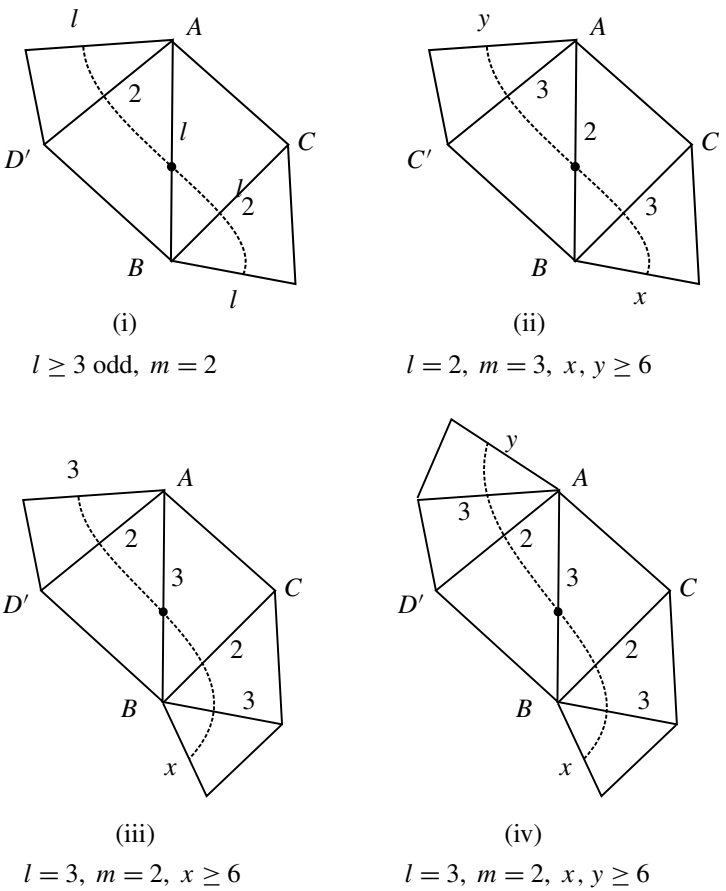

Figure 31. After further analysis, applied to the cases of Figure 29, these are the remaining cases of Figure 19(c) to consider.

Figure 31(i). This change is due to the fact that, when l is even, the edge label 2 for AD' in 31(i) must equal the edge label for AC. However, this would contradict our assumption that none of the vertices of T is finite, because C would have two incident edges, AC and BC, labeled 2.

So we are left to analyze the cases of Figure 31. We begin with case (iv). See Figure 32. The multiple parts of this figure are explained in the caption. Referring to the left side of the lower half of the figure, Π_1 is the plane through edge AC'' inclined closest to the switch edge AB and Π_2 is the plane through edge BD''

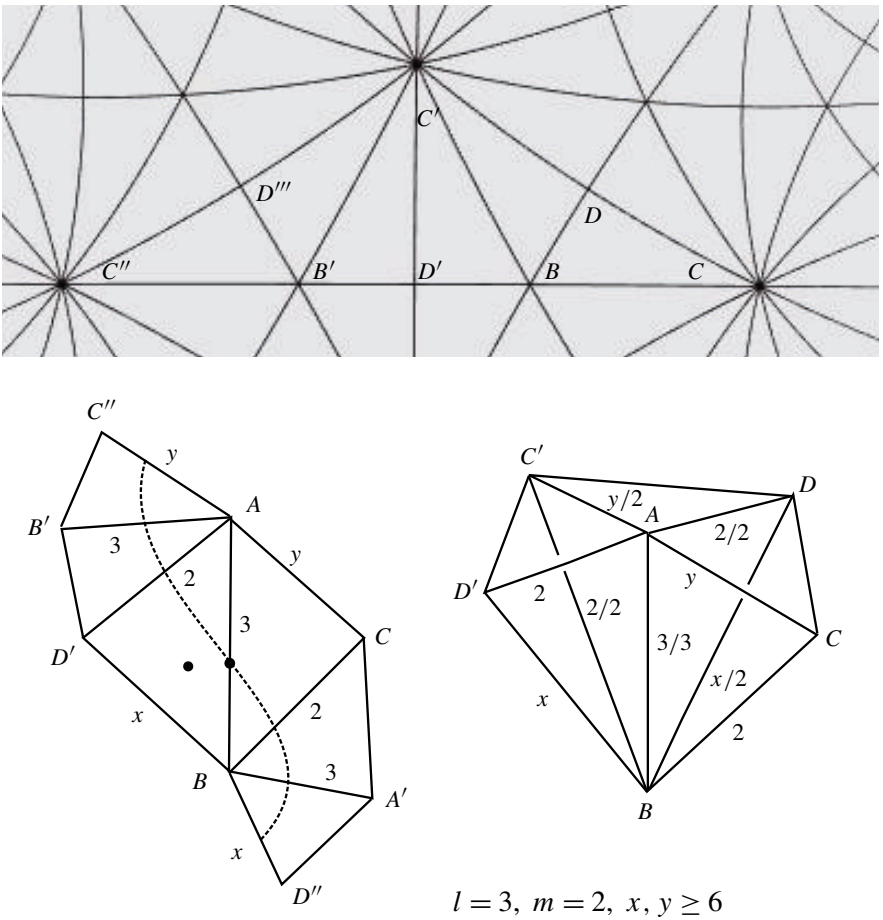

Figure 32. The case of Figure 31(iv). The upper half of the figure represents the view from the vertex A when $y = 7$. The lower half consists of a perspective image of the three copies of the tetrahedron $ABCD$ on the right, and several triangles in the development of the face ABC on the left.

inclined closest to the switch edge AB. We wish to show that $\Pi_1 \cap \Pi_2 = \varnothing$. We do so using the upper half of the figure, which shows the view from A under the assumption that $y = 7$ (the same argument we give here applies to any other value for $y \geq 6$). In the upper half of the figure, the plane Π_1 is represented by the line $C''D'''$, and the plane ACD — which is depicted in the right side of the lower half of the figure, and which is the plane through AC inclined closest to the switch edge AB in the left side of the lower half of the figure — is represented by the line CD. Recalling that Π_F is the plane containing the face ABC (and, therefore, the plane in which the left side of the lower half of the figure is drawn, as well as the horizontal line in the upper half of the figure), we observe that there are two planes, other than Π_F, that pass through AB. These planes are represented in the upper half of the figure by the lines BC' and BD. Using the upper half of the figure, we observe that any point of Π_1 that is on the same side of ACD as the vertex B is also on the same side of the plane ABC' (which is represented by the line BC') as the point D'. We now use the previous case (Section 4.2.1) to observe that $\Pi_2 \cap ACD = \varnothing$: namely, Π_2 and ACD are the planes through BD'' and AC, respectively, inclined closest to the *new* switch edge BC for the three triangles ABC, $A'BC$ and $A'BD''$ from the lower left half of Figure 32, to which Section 4.2.1 applies (to see this more clearly, turn these three triangles together so that the edge BC is vertical, and compare with Figure 22). In exactly the same way (i.e., using Section 4.2.1), we see that $\Pi_2 \cap AC'D' = \varnothing$, this time using AB as the switch edge. But now, since Π_2 is on the same side of ACD as the vertex B *and* on the same side of $AC'D'$ as the vertex B, we can use the upper half of Figure 32 to see that there is no part of Π_1 which is both on the B side of $AC'D'$ *and* on the B side of ACD. Therefore, $\Pi_1 \cap \Pi_2 = \varnothing$.

The argument of the previous paragraph can be used in case (iii) of Figure 31. See Figure 33. In the lower left half of this figure, Π_1 is the plane through the edge AB' inclined closest to the switch edge AB. In the lower right half, Π_1 is the plane $AC'B'A''$. In the upper half of the figure, which represents the view from A when $y = 7$ (the case when $y \geq 6$ is similar), Π_1 is represented as the line $B'C'$. Proceeding as in the previous paragraph, we have $\Pi_2 \cap ACD = \Pi_2 \cap AC'D' = \varnothing$ (by Section 4.2.1). Furthermore, Π_2 is on the B side of both ACD and $AC'D'$. But now, referring to the upper half of Figure 33, we see that there is no part of Π_1 that is on the B side of both ACD and $AC'D'$. So $\Pi_1 \cap \Pi_2 = \varnothing$.

We now address case (ii) of Figure 31. See Figure 34. In the upper part of this figure, Π_1 and Π_2 are the planes through the edges AD' and BD'', respectively, that are inclined closest to the switch edge AB. In the lower part of the figure, which depicts the development of multiple copies of the tetrahedron, Π_1 is the plane $ADB'D'$ and Π_2 is the plane $BDA'D''$. Because these two planes are both incident to the nonfinite vertex D, they intersect if and only if their intersections

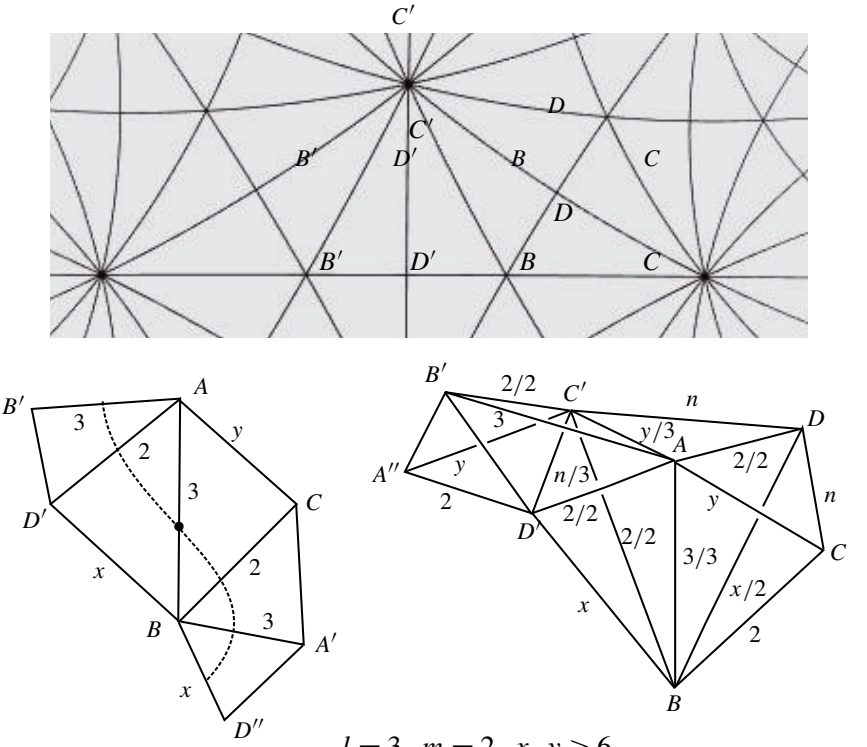

$l = 3,\ m = 2,\ x, y \geq 6$

Figure 33. The case of Figure 31(iii). The upper half of the figure represents the view from vertex A when $y = 7$. The right side of the lower half of the figure depicts the development of several copies of the tetrahedron, and the left side of the lower half depicts the development of the face ABC.

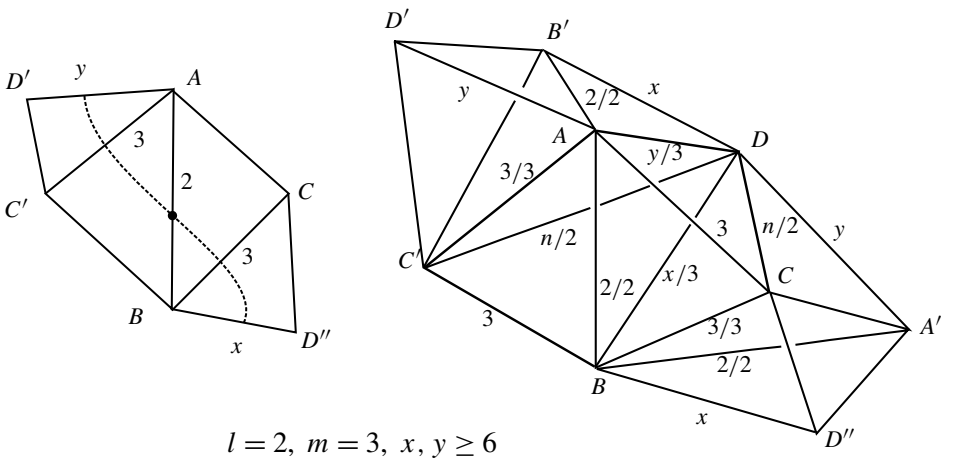

$l = 2,\ m = 3,\ x, y \geq 6$

Figure 34. The case of Figure 31(ii).

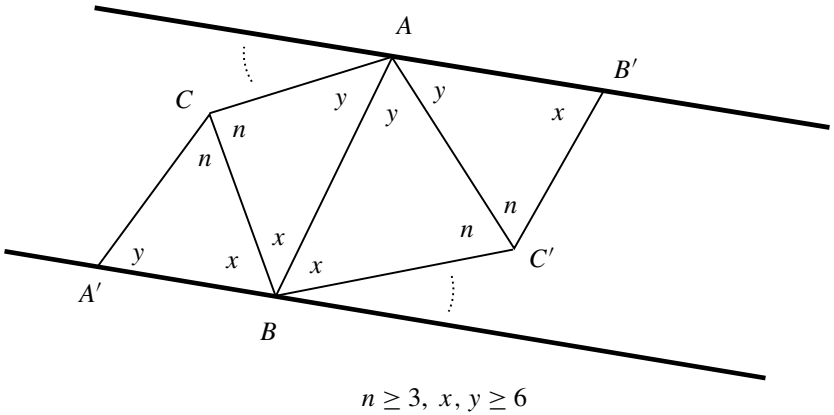

Figure 35. The schematic view from the vertex D for Figure 34. The letters x, y and n represent the integral submultiples of π of the dihedral angles of the tetrahedra incident at D.

with the link of D intersect. See Figure 35, which schematically depicts the view of this link from the vertex D.

In the figure, Π_1 is represented by the bold line AB' and Π_2 by the bold line $A'B$. We have labeled the interior angles of the triangles in this view by their submultiples of π. Because vertex C has two edges of order 3 incident to it, we must have that $n \geq 3$. But since x and y must both be at least 6, we can use Figure 21(iii) (with base the segment AB) to conclude that the bold lines cannot intersect on either side of the line AB. So $\Pi_1 \cap \Pi_2 = \varnothing$ in the case of Figure 31(ii).

This leaves case (i) of Figure 31. We begin by assuming that $l \geq 5$ (recall that l must be odd). See Figure 36, which depicts the view from the vertex A with the projection centered at the vertex B, and Figure 37. For the purposes of illustration, we take the type of A to be $(2, 4, 5)$, although the argument only depends on the

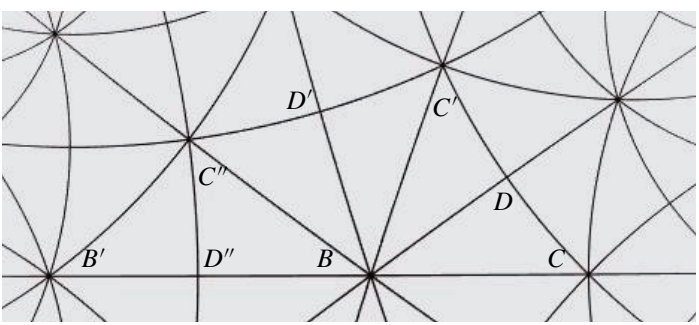

Figure 36. The case of Figure 31(i): view from the vertex A, in the case when A has type $(2, 4, 5)$.

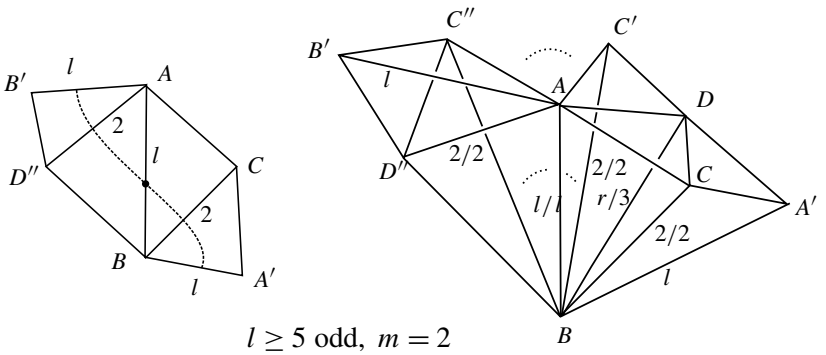

Figure 37. The case of Figure 31(i) (continued).

presence of the order 2 edge incident to A and the fact that the order of the edge AB is at least 5. The plane Π_1 is represented by the circular arc $B'C''$. We note that the plane $BC'D$ in the lower right part of the figure is represented in the upper half of the figure by a circle, centered on the line segment BC' because the planes $BC'D$ and ABC' are perpendicular, and whose interior disk does not contain any of the points B, D, C' or D'. As we have observed previously (see the argument depicted in Figure 15 from Section 4.1.3), the circle representing $BC'D$ can intersect at most two sides of the l-gon centered at B, and in this case those sides will always be $D'C'$ and DC'. It is clear that this circle is disjoint from the arc $B'C''$ representing Π_1, and hence that $\Pi_1 \cap BC'D = \varnothing$. Now referring to the lower right part of the figure, we observe that $\Pi_2 = A'BD$ (as planes) and that the part of Π_2 that is on the same side of BCD as A is also on the *opposite* side of $BC'D$ as A. Since Π_1 is disjoint both from $BC'D$ and BCD (the latter by the previous case of Section 4.2.1), and because Π_1 lies on the same side of these planes as A, we can conclude that $\Pi_1 \cap \Pi_2 = \varnothing$ in this case when $l \geq 5$.

So we now assume that $l = 3$ in this case. We are not able to use the argument of the previous paragraph because some of the intersections ruled out in the previous paragraph can occur in this case. We refer to Figure 38. The possible values for q, n and r in the figure are based on the fact that the tetrahedron has no finite vertices. In this figure, $\Pi_1 = AC'A''B'$ and $\Pi_2 = A'B''DB$ (as planes). We determine that these planes are disjoint by applying the techniques of Sections 4.1.1 and 4.1.2. In particular, if $n \geq 4$, then we use the geometry of the link of vertex C' to conclude that Π_1 is disjoint from the plane $BDC'D'$ (it lies to the same side of $BDC'D'$ as the vertex A) and the geometry of the link of vertex D to conclude that Π_2 is disjoint from the plane $ACDC'$ (it lies to the same side of $ACDC'$ as vertex B). Now by considering the plane ABD and the geometry of the vertex B, we have that the part of Π_2 that is on the C' side of ABD is always on the opposite side of $BDC'D'$ to

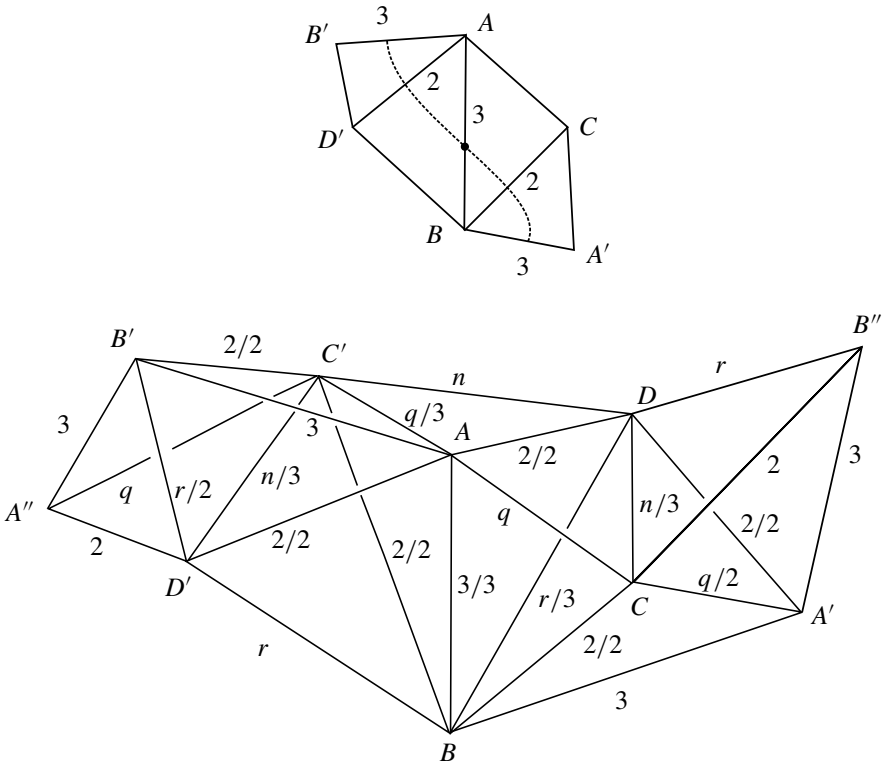

$$l = 3,\ m = 2,\ q, r \geq 6,\ n \geq 3$$

Figure 38. The case of Figure 31(i) when $l = 3$.

Π_1. Similarly, we have that the part of Π_1 on the D side of ABC' is always on the opposite side of $ACDC'$ to Π_2. We conclude that $\Pi_1 \cap \Pi_2 = \varnothing$. When $n = 3$, the argument is similar, except that $ACDC' = ACB''DC'$ and $BDC'D' = BDC'A''D'$ (as planes), and Π_1 and Π_2 will form interior angles on the B side of $ACB''DC'$ of $3\pi/q \leq \pi/2$ and $\pi/r \leq \pi/6$, respectively (so that Π_1 and Π_2 cannot intersect on the side of this plane opposite to B), and interior angles on the A side of $BDC'A''D'$ of $\pi/q \leq \pi/6$ and $3\pi/r \leq \pi/2$, respectively (so that Π_1 and Π_2 cannot intersection on the side of this plane opposite to A). Again, we conclude that $\Pi_1 \cap \Pi_2 = \varnothing$. This completes case (i) of Figure 31, and concludes this subsection.

4.2.3. *Figure 20(a):* See Figure 39, and recall the significance of the symbol * from the remark on page 224. We must first address the case when $e_2 = A^*C$. There are two possibilities that we must consider in determining whether or not Π_1 and Π_2 can intersect: either (1) Π_1 meets the plane through BC that is closest in inclination to the switch edge AB (it cannot meet more planes through BC, by our previous observations) and Π_2 meets at least the second closest plane through

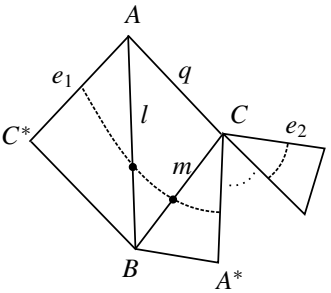

Figure 39. One case of Figure 20(a).

BC to the switch edge AB, or (2) Π_1 meets no planes passing through BC and Π_2 meets all of the planes passing through BC. We handle these two cases below:

(1) In order for Π_1 to meet a plane passing through BC, our tetrahedron must take one of the forms of items (1)–(3) in the summary at the conclusion of the paper. This follows from the extensive analysis of Section 4.1 (in fact, the pairwise intersections of Π_1, Π_F and the plane through BC inclined closest to the switch edge AB determine an immersed turnover in this case). We consider the case when $l = 3$, corresponding to item (3) in the summary. If $l = 3$, then $q = 2$, $m \geq 6$ and n (the order of the third edge associated to vertex C) is at least 3. It is then an easy analysis, using Figure 21 applied to the vertex C, to see that there is no choice of n and m for which Π_2 can intersect either of the two closest planes through BC toward the edge AB. So $\Pi_1 \cap \Pi_2 = \varnothing$. Exactly the same analysis holds if our tetrahedron takes the form of item (1) of the summary at the conclusion of the paper (in this case we have $l = 2$, $m \geq 6$, $n = 2$ and $q \geq 3$, and so the order of edge A^*C is either 2 or q, and there is no choice for m and q such that Π_2 meets either of the two planes through BC inclined closest to the switch). If our tetrahedron has the form of item (2) from the summary, then $l = 2$, $m \geq 3$ and $q \geq 6$. If m is odd and at least 5, then the order of edge A^*C is 2 and we can use Figure 21 applied to vertex C to conclude that Π_2 does not meet the two planes through BC inclined closest to the switch. If m is even and at least 6, then the order of A^*C is $q \geq 6$, and the conclusion of the previous sentence also holds. If $m = 4$, then we refer to Figure 40. Only the relevant edges are labeled in this figure, in which $\Pi_1 = AC^*D$ and $\Pi_2 = A^*D'A'C$. Because $q \geq 6$, we have that Π_1 and Π_2 form interior angles on the side of $ACA'D$ opposite to vertex B of $\pi/3$ and $(q-2)\pi/q \geq 2\pi/3$, respectively (these are interior angles with respect to the edge CD). Therefore, Π_1 and Π_2 do not intersect on the side of this plane opposite to B. But, as we have observed, $\Pi_1 \cap A'BC = \varnothing$. Since the part of Π_2 that is on the B side of $ACA'D$ is always on the opposite side

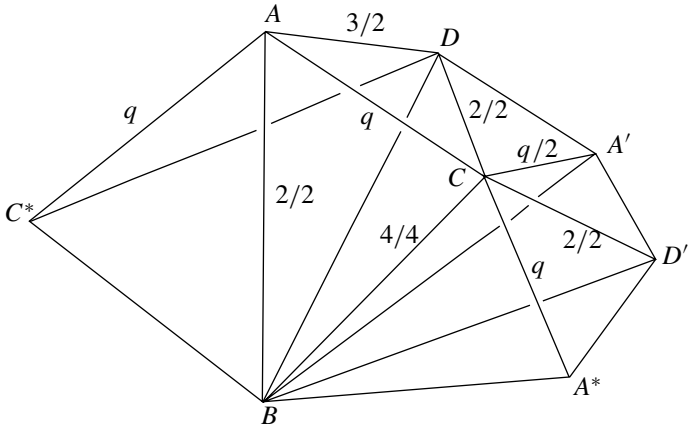

Figure 40. The case of Figure 39, when $l = 2$, $m = 4$ and $e_2 = A^*C$.

of $A'BC$ to Π_1, we have $\Pi_1 \cap \Pi_2 = \varnothing$. The case when $m = 3$ is exactly the same. These are all the possibilities for when the tetrahedron has one of the types (1)–(3) in the summary. So $\Pi_1 \cap \Pi_2 = \varnothing$ for this case.

(2) If the order of edge BC is greater than 4, then it is not possible to choose integers for the type of vertex C so that Π_2 crosses all the planes through BC. This follows by using the information of Figure 21 applied to the vertex C, as in the arguments that accompany Figure 23 in Section 4.2.1. The same statement is true (with the same argument) if the order of BC is 3 and the vertex C has no incident order 2 edge. So the order of edge BC is either 3 and C has the type $(2, 3, x \geq 6)$ or the order of edge BC is 2. Suppose that the edge BC has order 3. Then we can use the same argument as the one given at the end of the previous paragraph. Namely, it is readily shown that Π_1 and Π_2 meet the plane containing the face ACD at interior angles that sum to at least π on the opposite side of ACD of the vertex B, and since they do not meet on the B side of this plane, they must be disjoint. The same argument also works when the order of BC is 2. So $\Pi_1 \cap \Pi_2 = \varnothing$ in this case.

So we assume $e_2 \neq A^*C$. We observe that removing the sides AC^* and BC^* from the Figure 39 leaves a picture that is equivalent to the previous case of Section 4.2.1. We therefore know that Π_2 misses every plane through the switch edge AB. It follows, using Figure 21 applied to the vertex A, that l must be either 2 or 3, in order for Π_1 to cross every plane through this switch edge. Moreover, we must have, as in previous cases, that the type of vertices A and C must include an order 2 point. Suppose $l = 2$. This implies that neither m nor q is 2. If, in addition, neither m nor q is 3, then it is straightforward using the information in Figure 21 (applied to vertex C) to show that Π_2 cannot meet the plane through

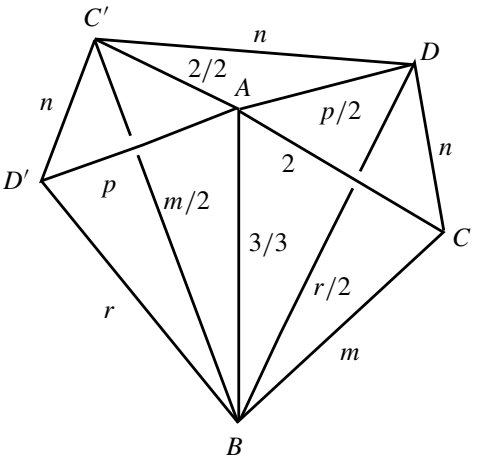

Figure 41. The case of Figure 39, when $l = 3$, $q = 2$ and $p \geq 6$.

A^*C inclined closest to Π_1, and so prove that $\Pi_1 \cap \Pi_2 = \varnothing$ in this case. So either $m = 3$ and $q \geq 6$ or $q = 3$ and $m \geq 6$, and in both cases $n = 2$. In either case, it is a straightforward application of the techniques already employed — specifically, the techniques involving developing tetrahedra from Sections 4.1.1 and 4.1.2 — to show that Π_1 and Π_2 do not intersect.

Now suppose $l = 3$. This implies that the order of edge e_1 is p. Because Π_1 must cross every plane through the switch edge AB, it is easily shown using Figure 21 (applied to vertex A) that the order p of edge e_1 is at least 6 and $q = 2$. Figure 41 shows three copies of T, with C^* relabeled as D'. Because $q = 2$, we must have $n \geq 3$ and $m \geq 3$. Since $n \neq 2$, analysis using the vertex D shows that Π_1, which is the plane $ADC'D'$, intersects the plane BCD if and only if $r = 2$. We analyze two cases:

Case $r \neq 2$: In this case, Π_1 does not intersect BCD, and so it is necessary for Π_2 to intersect BCD if Π_1 and Π_2 are to intersect. If $m \geq 4$ and even, then the edges emanating from the vertex C in Figure 39 — CA, CB, CA^*,..., e_2 — have labels that alternate $2, m, 2, \ldots$. However, by using Figure 30(ii) applied to the vertex C, it is easily seen that no plane through any of the edges CA^*,..., e_2 that is inclined closest to the switch edge AB will intersect the plane BCD. Since Π_1 does not intersect BCD, the latter plane separates Π_1 from Π_2. So we are left to consider when $m \geq 3$ and odd. When $m \geq 5$ and odd, an application of the information from Figure 21 to the vertex C shows that no plane that is inclined closest to the switch edge AB through any of the edges from CA^* to e_2 can intersect with the plane BCD. So again, $\Pi_1 \cap \Pi_2 = \varnothing$. Finally, when $m = 3$, it is necessary for n (the label of the third edge of T that meets the vertex C, and the label of the edge

CA^*) to be at least 6. So the type of the vertex C is $(2, 3, n \geq 6)$, and no plane through any edge after CA^* and up to and including e_2 that is inclined closest to the switch edge AB will intersect the closest such inclined plane through the edge CA^* (as in Figure 30(i)). Since, by the observation of the first paragraph of this section, the closest inclined plane to the switch edge AB through CA^* is disjoint from Π_1, we again have $\Pi_1 \cap \Pi_2 = \varnothing$. This completes the analysis of the case when $r \neq 2$.

Case $r = 2$*:* In this case, Π_1 does intersect the plane BCD. Because $r = 2$ and $l = 3$, it is necessary that $m \geq 6$. We have previously observed that Π_1 cannot intersect with the second-closest inclined plane to the switch edge AB through BC (because the planes Π_1, ABC and BCD form pairwise angles of intersection π/p, π/m and π/n, with $p \geq 6$, $m \geq 6$ and $n \geq 3$). However, vertex C has type $(2, m \geq 6, n \geq 3)$, and it is easily seen using the information of Figure 21 applied to C that no plane that is inclined closest to the switch edge AB through any of the edges from CA^* to e_2 can intersect the second-closest inclined plane to AB through CB, *provided* that $m \geq 7$. So this second-closest inclined plane through CB separates Π_1 from Π_2, when $m \geq 7$. This leaves the case when $m = 6$. But this case is handled by an argument similar to the accompanying argument for Figure 26 in Section 4.2.1. This completes the case when $r = 2$, and concludes this subsection.

4.2.4. *Figure 20(b):* See Figure 42. By the result of Section 4.2.1, it is not possible for e_2 to equal CA^*. Because of this, it is not possible, also by the Section 4.2.1, for Π_2 to meet any of the planes through the edge AB. Nor is it possible, by Section 4.2.1, for Π_1 to meet any of the planes through the edge BC. Consequently, the intersection of Π_1 and Π_2 can only occur if Π_1 crosses every plane through AB and Π_2 crosses every plane through BC. The subsequent possibilities and arguments to rule them out are all straightforward to carry out, using the techniques we have employed to this point. This completes the proof of Theorem 1.2. □

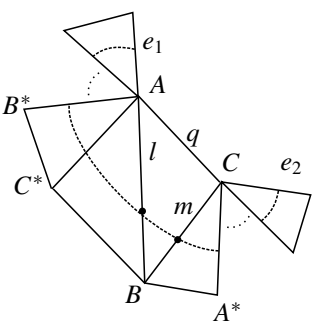

Figure 42. One case of Figure 20(b).

Summary

We provide a summary of the classification of immersed turnovers in the orbifold $\mathbb{O}_T$ associated to the generalized tetrahedron $T[l, m, q; n, p, r]$. These are listed in the order in which they appear in the proof, but isometric cases are indicated (the 24 isometric cases are determined by applying an element of the symmetric group S_4: any element of the symmetric group S_3 may be applied to both the first and second triples of $T[l, m, q; n, p, r]$, and any pair from one triple may be swapped with the corresponding pair of the other triple). We also include a conjectural list of all the immersed turnovers in hyperbolic tetrahedral orbifolds. All of these can be confirmed using the techniques of this paper, and while the author believes this list to be exhaustive, the necessary computations to determine the complete classification are somewhat extensive.

(1) $T[2, m, q; 2, p, 3]$. $\mathbb{O}_T$ contains an immersed (q, m, p) turnover, where $q \geq 3$, $m \geq 6$ and $p \geq 6$.

(2) $T[2, m, q; 2, 3, r]$ (isometric to item (1)). $\mathbb{O}_T$ contains an immersed (q, m, r) turnover, where $q \geq 6$, $m \geq 3$ and $r \geq 6$.

(3) $T[3, m, 2; n, p, 2]$ (isometric to item (1)). $\mathbb{O}_T$ contains an immersed (m, n, p) turnover, where $m \geq 6$, $n \geq 3$ and $p \geq 6$.

Conjectural list of all immersed turnovers in hyperbolic tetrahedral orbifolds:

(4) $T[2, m, q; 2, p, 3]$. $\mathbb{O}_T$ contains an immersed (q, m, p) turnover for any of the following values:

  (a) $q = 2$, $m = 4$ and $p \geq 5$. In this case, $\mathbb{O}_T$ also contains
    (i) a $(2, p, p)$ turnover,
    (ii) a $(4, 4, 5)$ turnover if $p = 5$, and
    (iii) a $(p/2, p, p)$ turnover if p is even.

  (b) $q = 2$, $p = 4$ and $m \geq 5$ (isometric to item (4), with the same set of additional nonmaximal turnovers).

  (c) $q = 2$, $m \geq 5$ and $p \geq 5$. In this case, $\mathbb{O}_T$ also contains
    (i) a $(m, m, p/2)$ turnover if p is even, or
    (ii) a $(m/2, p, p)$ turnover if m is even.

  (d) q, m and p are all greater than 2, and at least one is greater than 3. In this case, if two of the values are 3, then $\mathbb{O}_T$ also contains a (x, x, x) turnover, where x is the integer that is greater than 3.

(5) $T[3, 2, 2; 2, p, 3]$. $\mathbb{O}_T$ contains an immersed $(2, p, p)$ turnover, where $p \geq 5$.

(6) $T[3, m, 2; 2, p, 3]$. $\mathbb{O}_T$ contains an immersed (m, p, p) turnover, where $m \geq 3$ and $p \geq 4$.

(7) $T[3, m, 3; 2, 3, 2]$. $\mathbb{O}_T$ contains an immersed $(3, m, m)$ turnover, where $m \geq 4$.

(8) $T[4, 3, q; 2, 2, 2]$. $\mathbb{O}_T$ contains an immersed $(q, q, 3)$ turnover, where $q \geq 4$.

(9) $T[2, 2, 4; n, 3, r]$. $\mathbb{O}_T$ contains an immersed turnover of type $(2, 4, r \geq 5)$ (as well as the additional nonmaximal turnovers listed in item (4)) if $n = 2$, an immersed turnover of type $(4, 4, r \geq 3)$ if $n = 3$, and immersed turnovers of types $(3, 3, 5)$, $(3, 5, 5)$ and $(5, 5, 5)$ if $n = 2$ and $r = 5$.

(10) $T[2, 3, q; 2, 3, r]$. $\mathbb{O}_T$ contains an immersed (q, r, r) turnover, where $q \geq 3$ and $r = 4$ or $r = 5$.

(11) $T[2, 2, q; 3, 5, 2]$. $\mathbb{O}_T$ contains an immersed $(q, q, 5)$ turnover, where $q \geq 3$.

(12) $T[2, 2, 5; 2, 3, 5]$. $\mathbb{O}_T$ contains an immersed $(3, 5, 5)$ turnover.

(13) $T[2, 2, 3; 3, p, 2]$. $\mathbb{O}_T$ contains immersed turnovers of type $(3, p, p)$ and (p, p, p), where $p = 5$ or $p = 6$ (also, $(2, p, p)$ by item (5) and $(3, 3, 5)$, when $p = 5$, by item (11)).

(14) $T[2, 2, 3; 2, p, 3]$. $\mathbb{O}_T$ contains immersed turnovers of type $(2, p, p)$, $(3, 3, p)$ and (p, p, p) if $p = 5$, and an immersed turnover of type $(3, p, p)$ if $p = 6$.

Acknowledgments

The author thanks Ian Agol for helpful conversations. Very special thanks to the referee for invaluable feedback and for recommending simplifications to some of the arguments.

References

[Adams and Schoenfeld 2005] C. Adams and E. Schoenfeld, "Totally geodesic Seifert surfaces in hyperbolic knot and link complements. I", *Geom. Dedicata* **116** (2005), 237–247. MR 2006j:57008 Zbl 1092.57003

[Andreev 1970a] E. M. Andreev, "On convex polyhedra in Lobachevskii spaces", *Mat. Sb.* (*N.S.*) **81** (1970), 445–478. In Russian; translated in *Math. USSR Sb.* **10** (1970), 413-440. MR 41 #4367 Zbl 0217.46801

[Andreev 1970b] E. M. Andreev, "On convex polyhedra of finite volume in Lobachevskii space", *Mat. Sb.* (*N.S.*) **83** (1970), 256–260. In Russian; translated in *Math. USSR Sb.* **12** (1971), 255-259. MR 42 #8388

[Boileau et al. 2003] M. Boileau, S. Maillot, and J. Porti, *Three-dimensional orbifolds and their geometric structures*, Panoramas et Synthèses **15**, Société Mathématique de France, Paris, 2003. MR 2005b:57030 Zbl 1058.57009

[Cooper et al. 2000] D. Cooper, C. D. Hodgson, and S. P. Kerckhoff, *Three-dimensional orbifolds and cone-manifolds*, MSJ Memoirs **5**, Math. Soc. of Japan, Tokyo, 2000. MR 2002c:57027 Zbl 0955.57014

[Dunbar 1988] W. D. Dunbar, "Hierarchies for 3-orbifolds", *Topology Appl.* **29**:3 (1988), 267–283. MR 89h:57008 Zbl 0665.57011

[Hodgson 1992] C. D. Hodgson, "Deduction of Andreev's theorem from Rivin's characterization of convex hyperbolic polyhedra", pp. 185–193 in *Topology '90*, edited by B. Apanasov et al., Ohio State Univ. Math. Res. Inst. Publ. **1**, de Gruyter, Berlin, 1992. MR 93h:57022 Zbl 0765.52013

[Maclachlan 1996] C. Maclachlan, "Triangle subgroups of hyperbolic tetrahedral groups", *Pacific J. Math.* **176**:1 (1996), 195–203. MR 98d:20056 Zbl 0865.20031

[Maskit 1988] B. Maskit, *Kleinian groups*, Grundlehren der Mathematischen Wissenschaften **287**, Springer, Berlin, 1988. MR 90a:30132 Zbl 0627.30039

[Morgan 1984] J. W. Morgan, "On Thurston's uniformization theorem for three-dimensional manifolds", pp. 37–125 in *The Smith conjecture* (New York, 1979), edited by J. W. Morgan and H. Bass, Pure Appl. Math. **112**, Academic Press, Orlando, FL, 1984. MR 758464 Zbl 0599.57002

[Rafalski 2010] S. Rafalski, "Immersed turnovers in hyperbolic 3-orbifolds", *Groups Geom. Dyn.* **4**:2 (2010), 333–376. MR 2011a:57036 Zbl 1194.57024

[Ratcliffe 1994] J. G. Ratcliffe, *Foundations of hyperbolic manifolds*, Graduate Texts in Mathematics **149**, Springer, New York, 1994. MR 95j:57011 Zbl 0809.51001

[Roeder et al. 2007] R. K. W. Roeder, J. H. Hubbard, and W. D. Dunbar, "Andreev's theorem on hyperbolic polyhedra", *Ann. Inst. Fourier* (*Grenoble*) **57**:3 (2007), 825–882. MR 2008e:51011 Zbl 1127.51012

[Singerman 1972] D. Singerman, "Finitely maximal Fuchsian groups", *J. London Math. Soc.* (2) **6** (1972), 29–38. MR 48 #529 Zbl 0251.20052

[Thurston 1979] W. P. Thurston, "The geometry and topology of three-manifolds", lecture notes, Princeton University, 1979, available at http://msri.org/publications/books/gt3m.

[Thurston 1982] W. P. Thurston, "Three-dimensional manifolds, Kleinian groups and hyperbolic geometry", *Bull. Amer. Math. Soc.* (*N.S.*) **6**:3 (1982), 357–381. MR 83h:57019 Zbl 0496.57005

[Thurston 1997] W. P. Thurston, *Three-dimensional geometry and topology*, vol. 1, Princeton Mathematical Series **35**, Princeton Univ. Press, Princeton, NJ, 1997. MR 97m:57016 Zbl 0873.57001

[Ushijima 2006] A. Ushijima, "A volume formula for generalised hyperbolic tetrahedra", pp. 249–265 in *Non-Euclidean geometries: János Bolyai memorial volume* (Budapest, 2002), edited by A. Prékopa and E. Molnár, Math. Appl. (N. Y.) **581**, Springer, New York, 2006. MR 2007h:52008 Zbl 1096.52006

[Weeks $\geq$ 2012] J. Weeks, "Kaleidotile", available at http://www.geometrygames.org/KaleidoTile.

Received February 1, 2011. Revised October 28, 2011.

SHAWN RAFALSKI
DEPARTMENT OF MATHEMATICS AND COMPUTER SCIENCE
FAIRFIELD UNIVERSITY
1073 NORTH BENSON ROAD
15 BANNOW SCIENCE CENTER
FAIRFIELD, CT 06825-5195
UNITED STATES

srafalski@fairfield.edu

PACIFIC JOURNAL OF MATHEMATICS

http://pacificmath.org

Founded in 1951 by
E. F. Beckenbach (1906–1982) and F. Wolf (1904–1989)

See inside back cover or pacificmath.org for submission instructions.

The subscription price for 2012 is US $420/year for the electronic version, and $485/year for print and electronic.
Subscriptions, requests for back issues from the last three years and changes of subscribers address should be sent to Pacific Journal of Mathematics, P.O. Box 4163, Berkeley, CA 94704-0163, U.S.A. Prior back issues are obtainable from Periodicals Service Company, 11 Main Street, Germantown, NY 12526-5635. The Pacific Journal of Mathematics is indexed by Mathematical Reviews, Zentralblatt MATH, PASCAL CNRS Index, Referativnyi Zhurnal, Current Mathematical Publications and the Science Citation Index.

The Pacific Journal of Mathematics (ISSN 0030-8730) at the University of California, c/o Department of Mathematics, 969 Evans Hall, Berkeley, CA 94720-3840, is published monthly except July and August. Periodical rate postage paid at Berkeley, CA 94704, and additional mailing offices. POSTMASTER: send address changes to Pacific Journal of Mathematics, P.O. Box 4163, Berkeley, CA 94704-0163.

PJM peer review and production are managed by EditFLOW™ from Mathematical Sciences Publishers.

PUBLISHED BY PACIFIC JOURNAL OF MATHEMATICS
at the University of California, Berkeley 94720-3840
A NON-PROFIT CORPORATION
Typeset in LaTeX

PACIFIC JOURNAL OF MATHEMATICS

Volume 255 No. 1 January 2012